

# 1 **Modeling considerations for research on Ocean Alkalinity Enhancement** 2 **(OAE)**

3 Katja Fennel<sup>1</sup>, Matthew C. Long<sup>2</sup>, Christopher Algar<sup>1</sup>, Brendan Carter<sup>3</sup>, David Keller<sup>4</sup>, Arnaud  
4 Laurent<sup>1</sup>, Jann Paul Mattern<sup>5</sup>, Ruth Musgrave<sup>1</sup>, Andreas Oschlies<sup>4</sup>, Josiane Ostiguy<sup>1</sup>, Jaime B.  
5 Palter<sup>6</sup>, Daniel B. Whitt<sup>7</sup>

6  
7 Correspondence to: Katja Fennel, katja.fennel@dal.ca

8  
9 <sup>1</sup>Department of Oceanography, Dalhousie University, Halifax, Nova Scotia, Canada

10 <sup>2</sup>National Center for Atmospheric Research, University Corporation for Atmospheric Research,  
11 Boulder, Colorado, USA

12 <sup>3</sup>Pacific Marine Environmental Laboratory, National Oceanic and Atmospheric Association,  
13 Seattle, Washington, USA

14 <sup>4</sup>Marine Biogeochemical Modelling, GEOMAR Helmholtz Centre for Ocean Research Kiel, Kiel,  
15 Germany

16 <sup>5</sup>Ocean Sciences Department, University of California Santa Cruz, Santa Cruz, California, USA

17 <sup>6</sup>Graduate School of Oceanography, University of Rhode Island, Narragansett, Rhode Island,  
18 USA

19 <sup>7</sup>Earth Science Division, NASA Ames Research Center, Moffett Field, California, USA

## 20 21 **Abstract**

22 The deliberate increase of ocean alkalinity (referred to as Ocean Alkalinity Enhancement or  
23 OAE) has been proposed as a method for removing CO<sub>2</sub> from the atmosphere. Before OAE can  
24 be implemented safely, efficiently, and at scale several research questions have to be addressed  
25 including: 1) which alkaline feedstocks are best suited and in what doses can they be added  
26 safely, 2) how can net carbon uptake be measured and verified, and 3) what are the potential  
27 ecosystem impacts. These research questions cannot be addressed by direct observation alone  
28 but will require skillful and fit-for-purpose models. This article provides an overview of the  
29 most relevant modeling tools, including turbulence-, regional- and global-scale biogeochemical  
30 models, and techniques including approaches for model validation, data assimilation, and  
31 uncertainty estimation. Typical biogeochemical model assumptions and their limitations are  
32 discussed in the context of OAE research, which leads to an identification of further  
33 development needs to make models more applicable to OAE research questions. A description  
34 of typical steps in model validation is followed by proposed minimum criteria for what  
35 constitutes a model that is fit for its intended purpose. After providing an overview of  
36 approaches for sound integration of models and observations via data assimilation, the  
37 application of Observing System Simulation Experiments (OSSEs) for observing system design  
38 is described within the context of OAE research. Criteria for model validation and  
39 intercomparison studies are presented. The article concludes with a summary of  
40 recommendations and potential pitfalls to be avoided.

## 42 1 Introduction

43 Ocean Alkalinity Enhancement (OAE) refers to the deliberate increase of ocean alkalinity, which  
44 can be realized either by removing acidic substances from or adding alkaline substances to  
45 seawater. OAE is receiving increasing attention as a method for removing CO<sub>2</sub> from the  
46 atmosphere; such methods are referred to as marine Carbon Dioxide Removal (mCDR)  
47 technologies (Renforth and Henderson, 2017). Natural analogues to OAE exist (Shubas et al.  
48 2023). An increase in the alkalinity of seawater leads to a repartitioning of its dissolved  
49 carbonate species with a shift toward bicarbonate and carbonate ions (Zeebe and Wolf-Gladrow  
50 2001, Renforth and Henderson 2017), leading to a reduction in the aqueous CO<sub>2</sub> concentration  
51 and thus the partial pressure of CO<sub>2</sub> ( $p\text{CO}_2$ ; Schulz et al. 2023). Since exchange of CO<sub>2</sub> between  
52 the ocean and atmosphere occurs when the surface ocean  $p\text{CO}_2$  is out of equilibrium with that of  
53 the atmosphere, a lowering of the ocean's  $p\text{CO}_2$  will lead to a net ingassing of atmospheric CO<sub>2</sub>  
54 (i.e., an increase in CO<sub>2</sub> uptake by the ocean or a decrease in outgassing due to OAE). This  
55 would increase the oceanic and decrease the atmospheric inventories of inorganic carbon, in  
56 other words, it would result in mCDR. In contrast to other mCDR technologies, OAE does not  
57 exacerbate ocean acidification (Ilyina et al. 2013). In fact, an increase in ocean alkalinity  
58 counteracts acidification, and while subsequent net uptake of atmospheric CO<sub>2</sub> largely restores  
59 pH to its pre-perturbation value, there is potential for OAE deployment to mitigate acidification  
60 impacts near injection sites (Mongin et al. 2021).

61 Several important research questions should be addressed before implementing OAE as an  
62 mCDR technology at scale. These include: 1) which alkaline substances are best suited and in  
63 what doses can they be added reliably while avoiding precipitation of calcium carbonate (which  
64 would decrease alkalinity and could result in runaway precipitation events), 2) how can  
65 changes in alkalinity and net carbon uptake be measured, verified, and reported (referred to as  
66 MRV; see Ho et al. 2023) to enable meaningful carbon crediting, and 3) what are the potential  
67 ecosystem impacts and how can harm to ecosystems be avoided or minimized while  
68 maximizing potential benefits. These research questions cannot be addressed by direct  
69 observation alone but will require an integration of observations and numerical ocean models  
70 across a range of scales. Skillful and fit-for-purpose models will be essential for addressing  
71 many OAE research questions including the MRV challenge, assessment of environmental  
72 impacts, and interpretation of natural analogs.

73 Ocean models are useful for a broad range of purposes, from idealized models for basic  
74 hypothesis testing of fundamental principles to realistic models for more applied uses (see  
75 primer on ocean biogeochemical models by Fennel et al. 2022). In the context of OAE research,  
76 this full range of models is applicable. For example, idealized models of particle-fluid  
77 interaction can inform us about dissolution and precipitation kinetics at the scale of particles,  
78 realistic local-scale models can inform us about nearfield processes in the turbulent  
79 environment around injection sites, and larger-scale regional or global ocean models can be  
80 used to support observational design for field experiments, to demonstrate possible verification  
81 frameworks, and to address questions about global-scale feedbacks on ocean biogeochemistry.  
82 A common objective of all these modeling approaches is to realistically simulate the spatio-

83 temporal evolution of the seawater carbon chemistry, including alkalinity and dissolved CO<sub>2</sub>,  
84 and attribute that evolution to physical, chemical, and biological processes. Models that are  
85 suitable for this purpose will provide spatial and temporal context for properties that can be  
86 observed (but at much sparser temporal and spatial coverage than a model can provide) as well  
87 as estimates of properties and fluxes that cannot be directly observed but may be inferred  
88 because of known mechanistic relationships or patterns of correlation. Applications of realistic  
89 models rely on them being skillful and accurate, requiring that they include parameterizations  
90 of the relevant processes, and that they are constrained by observations that contain sufficient  
91 meaningful information (what is sufficient depends on the application and research question).  
92 Methods for constraining models by observations through statistically optimal combination of  
93 both are available. Application of such methods is referred to as data assimilation and provides  
94 the most accurate estimates of biogeochemical properties and fluxes (see Fennel et al. 2022 for  
95 fundamentals and code examples).

96 Model applications for OAE research include the following four general types:

- 97 • Hindcasts are model applications where a defined time period in the past was  
98 simulated. They can be unconstrained—in the sense that no observations are fed into the  
99 model except for initial, boundary, and forcing conditions—or constrained, where  
100 observations inform the model state via data assimilation. The latter are also referred to  
101 as optimal hindcasts or reanalyses.
- 102 • Nowcasts/forecasts are similar to constrained hindcasts but with the simulations carried  
103 out up to the present (referred to as nowcasts) or into the future (referred to as  
104 forecasts). The latter require assumptions about future forcing and boundary conditions,  
105 e.g., from other forecasts, climatology, or assuming persistence.
- 106 • Scenarios are unconstrained hindcasts or forecasts where one or more aspects of the  
107 model is systematically perturbed to assess the effect of the perturbation, for example, in  
108 paired simulations with and without OAE, one would be the realistic case and the other  
109 a scenario (also referred to as counterfactual in this case). These can be used to explore  
110 even very unlikely situations, which is often required in comprehensive uncertainty and  
111 risk assessment.
- 112 • Observing System Simulation Experiments (OSSEs) for observing system design use  
113 unconstrained and/or constrained hindcasts to evaluate the benefits of different  
114 sampling designs and optimize deployment of observational assets for a defined  
115 objective, including tradeoffs between different types of observation platforms.

116 Successful implementation of models to support OAE research and MRV is challenging because  
117 of the general sparseness of relevant biogeochemical observations, and the limited lab,  
118 mesocosm, and field trial data available to date for model parameterization. Further, models are  
119 built at a process level and integrated to reveal behavior at the emergent scale. As such, models  
120 comprise a collective hypothesis of the ocean's physical, biogeochemical, and ecosystem  
121 function—but it is important to recognize that model formulations of key processes related to

122 OAE remain uncertain. It may well turn out that parameterizations of the carbonate system, of  
123 plankton diversity and trophic interactions, small scale turbulence, submesoscale subduction  
124 and restratification processes, and air-sea gas exchange in the current generation of models  
125 require improvement to robustly treat OAE-related questions.

126 The intended scope of this article is to provide an overview of the most relevant modeling tools  
127 for OAE research with high-level background information, illustrative examples, and references  
128 to more in-depth methodological descriptions and further examples. We aim to provide simple  
129 criteria and guidance for researchers on the current state-of-the-art of biogeochemical modeling  
130 relevant to OAE research, keeping in mind short-term research goals in support of pilot  
131 deployments of OAE and long-term goals such as credible MRV in an ocean affected by large-  
132 scale deployment of OAE and possibly other CDR technologies.

## 133 **2 Modeling approaches**

134 This section provides a brief review of modeling tools available for OAE research with  
135 references to more in-depth methodological descriptions and examples, as well as a discussion  
136 of which approaches are most applicable to simulating essential processes in different  
137 circumstances. The presentation is structured using two complementary organizing principles,  
138 the spatial and temporal scales of the problem in Section 2.1 and the biogeochemical and  
139 ecological complexity represented by different modeling approaches in Section 2.2. Section 2  
140 concludes with a summary of suggested future model development efforts in Section 2.3.

141

### 142 **2.1. Modeling approaches across scales**

143 In the nearfield, close to the site of an alkalinity increase, an accurate characterization of the  
144 spatio-temporal evolution of alkalized waters requires direct representation or parameterization  
145 of fluid and particle physics and seawater carbonate chemistry at scales ranging from  
146 micrometers to hundreds of meters, spanning turbulent to submesoscale processes (Section  
147 2.1.1). In the farfield, covering scales from 10s of meters to 100s of kilometers, where the effect of  
148 an alkalinity increase depends less on the details of how the alkalinity was added, or acidity  
149 removed, and is instead dominated by ambient environmental processes, local to regional scale  
150 models are useful for simulating the impact of alkalinity increases, for verifying the intended  
151 perturbations in air-sea exchange of CO<sub>2</sub> and in carbonate system variables, and potentially for  
152 simulating ecosystem impacts (Section 2.1.2). Lastly, investigation of the effects of the global  
153 ocean's overturning circulation, impacts on atmospheric CO<sub>2</sub> levels, and of Earth system  
154 feedbacks resulting from deployment of OAE and other CDR technology at scale requires  
155 global modeling approaches (Section 2.1.3).

156

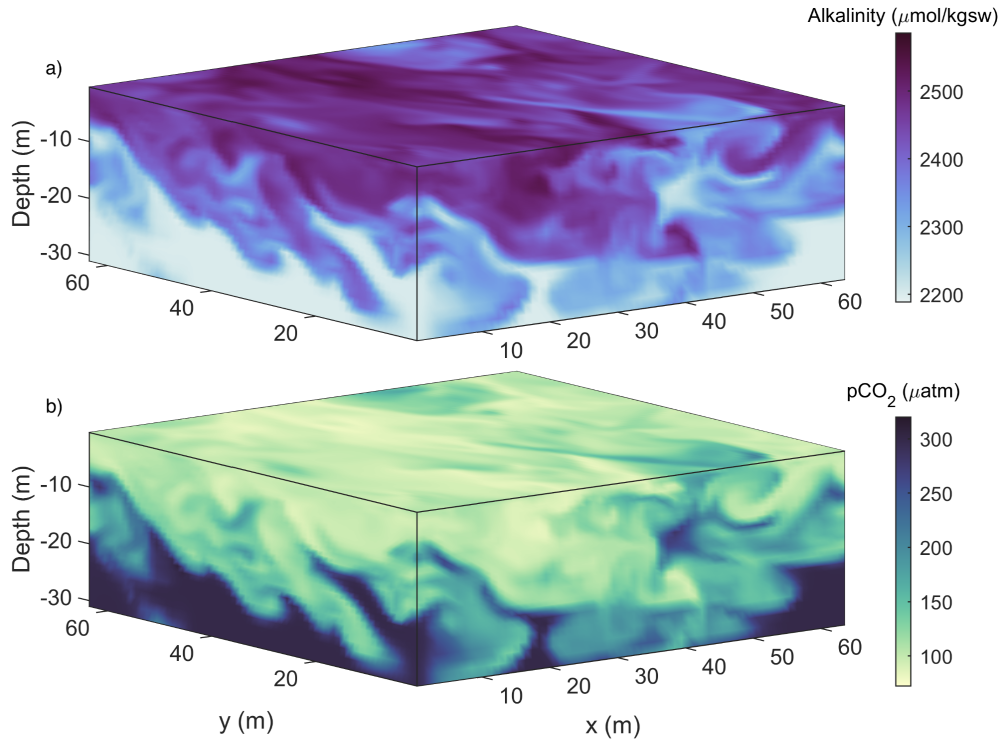
#### 157 **2.1.1. Particle scale to nearfield/turbulence scale ( $\mu\text{m}$ to km scales)**

158 Small-scale modeling approaches cover the range from  $\mu\text{m}$ -size particles to the turbulent- and  
159 submeso-scales in the nearfield of alkalinity additions. Simulating processes on these scales  
160 allows one to address questions about how turbulent mixing dilutes and disperses alkalized  
161 water and how it affects the settling, aggregation, disaggregation, precipitation, and dissolution

162 of suspended particles. Nearfield modeling has an important role to play in guiding the design  
163 of deployment strategies that mitigate environmental impacts and meet future permitting  
164 requirements, and to support monitoring. During the initial dispersion and dilution phase of an  
165 alkalinity increase in the nearfield, the direct impacts on carbonate system variables are  
166 greatest, with waters exhibiting the largest elevations in pH and the highest potential for the  
167 formation of secondary precipitates. For particulate alkalinity feedstocks, turbulence close to the  
168 deployment site affects dissolution and settling rates, increasing dissolution and either  
169 accelerating or diminishing the settling of sedimentary particles compared to the Stokes settling  
170 speed (Fornari et al. 2016).

171 Distinct approaches to modeling at these scales involve different levels of parametrization and  
172 computational expense, with the relative utility of each approach being dependent on the  
173 scientific questions at hand. At the smallest scales, Direct Numerical Simulations (DNS) are the  
174 most computationally expensive and specialized class of fluid modeling, as they resolve flows  
175 down to the scales at which flow variances dissipate—typically centimeters or smaller in the  
176 ocean. Consequently, computational constraints imply that they cannot be run over domains  
177 larger than a few meters. DNS are thus integrated over idealized physical domains (i.e., they  
178 lack realistic bathymetry) and are suited to investigating fundamental physical processes. For  
179 example, multiphase DNS simulations have been used to model the interaction of turbulence  
180 with gas bubbles (Farsoiya et al. 2023) and particles (Fornari et al. 2016). Results from such  
181 studies provide an important testbed that can be used to develop parameterizations required in  
182 lower resolution models.

183 A well-established approach to modeling the fluid flow at scales up to about 10 km uses Large  
184 Eddy Simulations (LES), a class of model that directly solves the unsteady Navier-Stokes  
185 equations down to the largest turbulent scales on a high-resolution grid. Such models  
186 parameterize turbulence using a subgrid-scale model (e.g., Smagorinsky 1963). An advantage of  
187 these models is their ability to simulate both an alkalized plume and the environmental  
188 turbulence into which the plume emerges. Once alkalized waters enter the surface boundary  
189 layer, LES models have an established history of simulating turbulence and mixing that is  
190 directly relevant to OAE research (e.g., Mensa et al. 2015, Taylor et al. 2020). An example of an  
191 LES simulation of near-surface turbulence dispersing surface-deployed alkalinity downwards is  
192 illustrated in Figure 1, where a physical model (Ramadhan et al. 2020) has been coupled to a  
193 carbonate solver (Lewis et al. 1998). To date, LES models have rarely been coupled to  
194 biogeochemical models due to the computational expenses involved, though their inclusion  
195 may be increasingly feasible (Smith et al. 2018, Whitt et al. 2019). As LES simulate flow physics  
196 at scales ranging from 10-10,000 m, they do not explicitly resolve the microscales of fluid motion  
197 and chemical reactions at particle scales. Nevertheless, the parameterizations of such processes  
198 can be included; for example, Liang et al. (2011) used models of bubble concentration and  
199 dissolved gas concentration in an LES to examine the influence of bubbles on air-sea gas  
200 exchange.



201 **Figure 1:** LES of near surface turbulence coupled to a carbonate system solver. Alkalinity is  
 202 added at a rate of  $4 \mu\text{mol kgsw}^{-1} \text{m}^{-2} \text{s}^{-1}$  for 20 minutes to the top grid cell at the start of the  
 203 simulation. Turbulence, generated by surface wind stress and cooling, sets the rate at which it  
 204 mixes downwards (a) along with associated waters of lowered  $p\text{CO}_2$  (b). Turbulent plumes and  
 205 eddies lead to inhomogeneities in water properties at scales of tens of meters.  
 206

207  
 208 For alkalized plumes associated with outfalls from, for example, wastewater treatment plants,  
 209 integral models (that assume plume properties such that the governing equations are  
 210 simplified) have been developed to examine the initial dilution close to jets and buoyant plumes  
 211 up to kilometer scales (Jirka et al. 1996). These models are highly configurable, enabling specific  
 212 diffuser configurations as well as the potential to incorporate sediment laden plumes with  
 213 particle settling (Bleninger & Jirka 2004). Results are commonly accepted for engineering  
 214 purposes, defining mixing zones, and providing a fast “first look” at diffusion and mixing near  
 215 an outfall site. However, these models rely on assumptions about the underlying physics of  
 216 fluid flow (e.g., axisymmetric plumes and simplified entrainment rates) that may not be  
 217 accurate under general oceanic conditions, and results will not include all effects of irregular  
 218 bathymetry, finite domain size or arbitrarily non-uniform ambient conditions. Nevertheless,  
 219 their simplicity makes them very useful. For example, by combining several simple process  
 220 models for plume dilution, particle dissolution, and carbon chemistry, Caserini et al. (2021)  
 221 have simulated the initial dilution of slaked lime  $\text{Ca}(\text{OH})_2$  particles and alkalinity in a plume  
 222 behind a moving vessel.

223 Other methods for modeling at this scale include Reynolds Averaged Navier Stokes (RANS)  
 224 and Unsteady RANS (URANS), wherein fluctuations against a slowly varying or time mean

225 background are parametrized, often using constant (large) eddy diffusivities and viscosities.  
226 These approaches are often inaccurate at these scales, resulting in simulations that are too  
227 diffusive or lacking processes that are of leading order importance to mixing (Golshan et al.  
228 2017, Chang & Scotti 2004).

229 There are multiple, potentially interacting sources of uncertainty to consider when evaluating  
230 the uncertainty of the applications described above. Perhaps best understood but still  
231 problematic is the uncertainty that arises from the computational intractability of simulating all  
232 the relevant scales in the  $\mu\text{m}$  to km range at once, necessitating the different modeling  
233 approaches for different scales, with parameterizations to account for unresolved scales and  
234 scale interactions. The dissolved carbonate chemistry of seawater is relatively well  
235 parameterized (Zeebe and Wolf-Gladrow 2001), but some modest uncertainties arise from  
236 approximations required for computational tractability (Smith et al. 2018). The least understood  
237 but potentially dominant source of uncertainty pertains to the representation of the microscale  
238 biological, chemical, and physical dynamics of particles, which is an active area of experimental  
239 and observational investigation (Subhas et al. 2022, Fuhr et al. 2022, Hartmann et al. 2023).  
240 While the explicit multiphase modeling of the particles themselves is computationally costly, an  
241 approach wherein the parametrized evolution of inertia-less Lagrangian particles are simulated  
242 may provide a fruitful middle ground, providing a mechanism to realistically determine the  
243 alkalinity release field associated with the advection, mixing, sinking and dissolution of reactive  
244 mineral particles. These questions about particles apply to those released in OAE deployments,  
245 as well as particles that precipitate from seawater in part due to OAE deployments, and finally  
246 the role of ambient biotic and abiotic particles where OAE is deployed.

247

### 248 **2.1.2. Local to regional scales (m to km)**

249 Local to regional scale models that range in horizontal resolution from tens of meters to  
250 hundreds of kilometers are useful for simulating the impact of alkalinity injections beyond the  
251 immediate local area, where conditions do not depend on the details of how the alkalinity was  
252 added and instead are determined by regional-scale currents and other process, including the  
253 potential for biogenic feedbacks. These models are particularly useful to support OAE field  
254 experiments, including planning and observational design, and analysis, integration and  
255 synthesis of observations, and to facilitate interpretation of observations from natural analogs.  
256 Furthermore, local and regional scale models will likely prove to be indispensable for  
257 quantification of OAE effects in research settings, for guiding assessments of its environmental  
258 impacts, and for MRV during the potential implementation of OAE. A skillful model can  
259 simulate when and where changes in carbonate chemistry and the ensuing anomalies in air-sea  
260  $\text{CO}_2$  exchange occur and provide an estimate of the spatio-temporal extent of the  
261 biogeochemical properties affected by OAE.

262

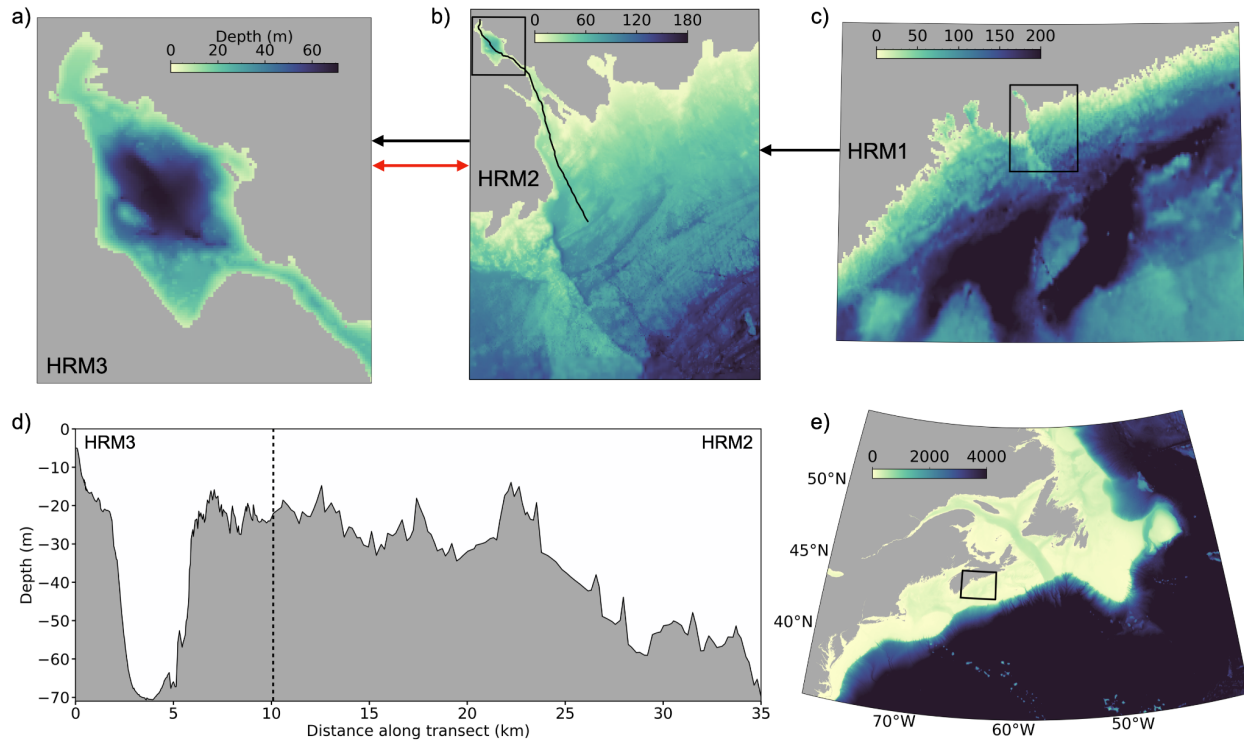
263 Regional models have distinct advantages over global models in their ability to resolve the  
264 spatial scales on which OAE would be applied both experimentally and operationally, and their  
265 documented skill in representing coastal and continental shelf processes more accurately  
266 (Mongin et al. 2016, Laurent et al. 2021). Examples of regional model applications in the context

267 of OAE include the recent studies by Mongin et al. (2021) and Wang et al. (2023). Mongin et al.  
268 (2021) used a coupled physical-biogeochemical-sediment model tailored to Australia's Great  
269 Barrier Reef to investigate to what extent realistic OAE applied along a shipping line could  
270 alleviate anthropogenic ocean acidification on the reef. Wang et al. (2023) used a coupled ice-  
271 circulation-biogeochemical model of the Bering Sea to study the efficiency of OAE in coastal  
272 Alaska.

273  
274 Implementation of a regional model in a target domain requires generation of a grid with  
275 associated bathymetry, specification of boundary conditions (including atmospheric forcing,  
276 information about ocean dynamics along the lateral boundaries of the domain, any fluxes of  
277 biogeochemical properties across the air-sea, sediment-water, and land-ocean boundaries, river  
278 inputs), and generation of initial conditions within the domain (Fennel et al. 2022). Different  
279 circulation models are available for implementation in domains targeted for OAE studies (see,  
280 e.g., Table 1 in Fennel et al. 2022), all with distinct strengths and established user communities.  
281 Particularly relevant in the context of studying coastal applications of OAE is a model's ability  
282 to accurately represent coastal topography, making unstructured grid models and models with  
283 terrain-following coordinates particularly attractive. Another feature to be considered is a  
284 model's ability to run in two-way nested configurations. In the more widely applied one-way  
285 nesting of domains, simulated conditions from a larger scale model (referred to as the parent  
286 model) are used to generate the dynamic lateral boundary conditions of a smaller scale, higher  
287 resolution model (the child model), which runs off line from the parent model. With two-way  
288 nesting, both models run simultaneously and information is exchanged continually along their  
289 intersecting boundaries. This allows information generated within the high-resolution child  
290 domain (e.g., the spreading distribution of a tracer or alkalinity addition) to be received and  
291 propagated by the larger-scale parent model. In this context, model simulations are particularly  
292 useful if available in near-real time or in forecast mode. This requires specification of lateral  
293 boundary conditions and atmospheric forcing up to the present and into the future. Global  
294 1/12th-degree nowcasts and 10-day forecasts of ocean conditions are available from the  
295 Copernicus Marine Service (CMEMS 2023) and atmospheric forcing up to the present and 10  
296 days into the future are available from the European Centre for Medium Range Weather  
297 Forecasts (ECMWF 2023).

298  
299 One example of a high-resolution local scale model with two-way nested domains is a  
300 framework developed for Bedford Basin in Halifax, Canada (Figure 2, Laurent et al. 2024). The  
301 model framework consists of three nested ROMS models (ROMS is the Regional Ocean  
302 Modelling System; <https://myroms.org>, Haidvogel et al. 2008, Shchepetkin and McWilliams  
303 2005). The outermost ROMS domain has a resolution of 900 m and is nested one-way within the  
304 data-assimilative global GLORYS reanalysis of physical and biogeochemical properties  
305 (Lellouche et al. 2021). Nested within are two models with increasingly higher resolutions of  
306 200 m and 60 m. Depending on the scientific objective to be addressed, the models can be run in  
307 one-way and two-way nested mode, where two-way nesting is computationally more  
308 demanding, and in hindcast or forecast mode. Implementation of dye-tracers within the model  
309 (Wang et al. 2024) allows one to determine dynamic distribution patterns and residence times.





310  
 311  
 312 **Figure 2:** Nested configuration of three ROMS models for the Bedford Basin and the adjacent  
 313 harbor in Halifax Regional Municipality (HRM). a) The highest resolution model (HRM3; 60 m)  
 314 includes the 7 km-long and 3 km-wide Bedford Basin and The Narrows, a 20-m shallow narrow  
 315 channel that connects the basin to the outer harbor. b) The larger scale model (HRM2, 200 m)  
 316 includes Bedford Basin and Halifax Harbor as well as the adjacent shelf. c) The largest-scale  
 317 model (HRM3, 900 m) covers the central part of the Scotian Shelf as indicated in e). d)  
 318 bathymetry along a section through HRM3 and HRM2, indicated by the black line in b). Lateral  
 319 boundaries of HRM3, HRM2, and HRM1 are shown by black boxes in b), c) and e), respectively.  
 320 Black arrows indicate the information flow between models in one way nesting mode. The red  
 321 arrow indicates that HRM1 and HRM2 can be run simultaneously with bi-directional flow of  
 322 information (two-way coupled mode).

323  
 324 **2.1.3. The global scale**

325 A strength of global ocean models is their capacity to comprehensively represent the global  
 326 overturning circulation and ocean ventilation. These processes control the time scales over  
 327 which waters are sequestered in the ocean interior and determine how long surface waters are  
 328 exposed to the atmosphere and can exchange properties, including CO<sub>2</sub>, before being injected  
 329 back into the ocean interior (Naveira Garabato et al. 2017). Similarly, the large-scale overturning  
 330 circulation and the patterns associated with ventilation are important to consider in the context  
 331 of deploying OAE at scale, as these patterns exert strong control on the efficiency of OAE at  
 332 sequestering CO<sub>2</sub> (e.g., Burt et al. 2021).

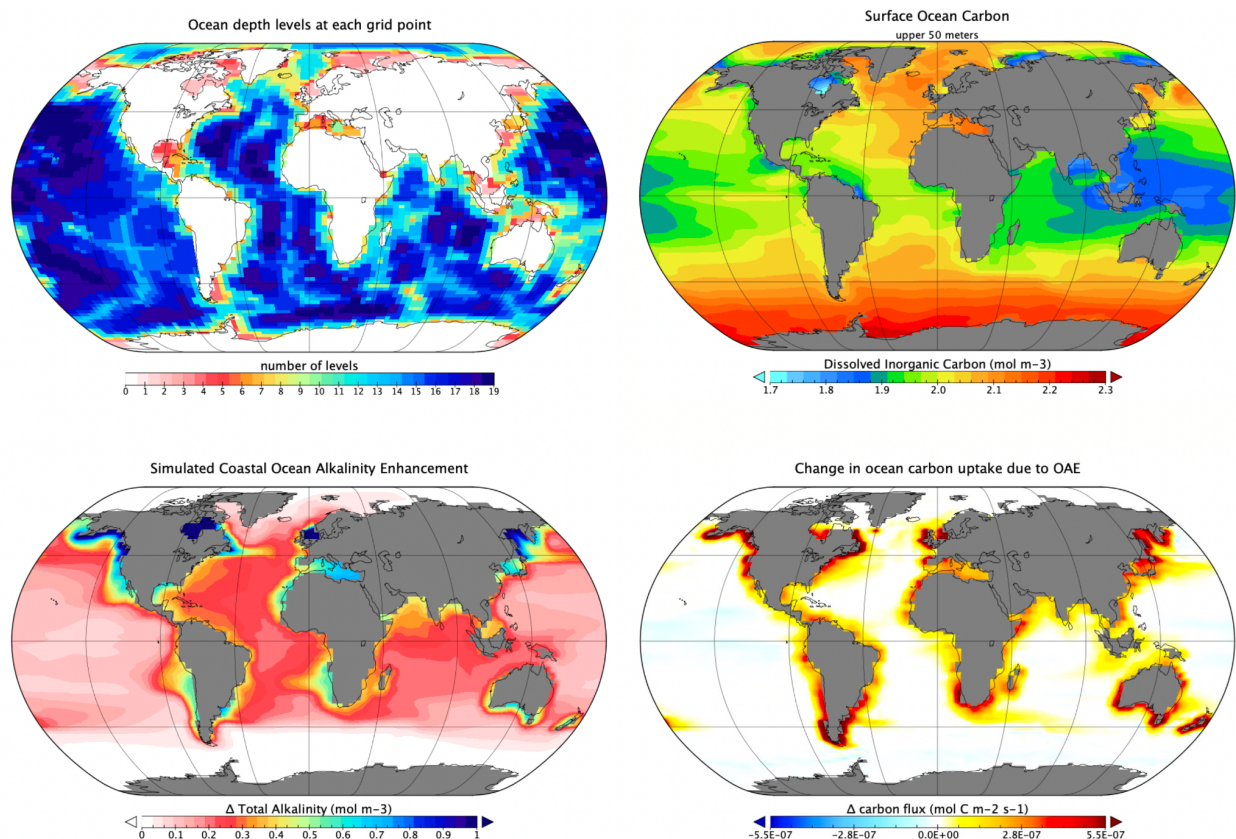
333 When global ocean models are dynamically coupled with models of the land biosphere and the  
334 atmosphere, they are referred to as Earth System Models (ESMs) and can be employed to  
335 explore Earth system feedbacks to mCDR. In the case of OAE, the main feedback is the change  
336 in atmospheric  $p\text{CO}_2$  and air-sea gas exchange that will result when CDR approaches are  
337 implemented at scale. While regional models have to be forced by atmospheric  $\text{CO}_2$   
338 concentrations, ESMs represent the atmospheric reservoir and are forced by  $\text{CO}_2$  emissions into  
339 the atmosphere, which then interacts with land and ocean carbon reservoirs. Only the latter  
340 approach can account for OAE-induced reductions in the atmospheric  $\text{CO}_2$  inventory which, in  
341 turn, would lead to a systematic reduction in air-sea  $\text{CO}_2$  fluxes. Regional models and global  
342 ocean models that do not explicitly represent the atmospheric  $\text{CO}_2$  reservoir and instead are  
343 forced by prescribed atmospheric  $p\text{CO}_2$  cannot simulate the decline in atmospheric  $p\text{CO}_2$  due to  
344 OAE. Depending on the alkaline material applied, there may also be feedbacks associated with  
345 changes in temperature, albedo, nutrient cycles, and biological responses which can be studied  
346 with the help of ESMs.

347 Another important strength of global models relates to the fact that anomalies in air-sea  $\text{CO}_2$   
348 flux generated by OAE deployments will manifest over large spatio-temporal scales because  
349  $\text{CO}_2$  equilibrates with the atmosphere via gas exchange slowly. Alkalinity enhanced waters can  
350 be transported far away from injection sites before equilibration is complete (He and Tyka  
351 2023). Consequently, OAE signals may exit the finite domain of regional models prior to full  
352 equilibration with the atmosphere (e.g., Wang et al. 2023). Because global models represent the  
353 entire ocean and can be integrated for centuries and longer, they enable full-scale assessments.

354 A primary challenge for global models, however, is that their horizontal resolution is  
355 necessarily limited by computational constraints (see example in Figure 3). Most of the global  
356 ocean models contributing the Coupled Model Intercomparison Project version 6 (CMIP6), for  
357 example, have horizontal resolutions of about  $1^\circ$  or roughly 100 km (Heuzé 2021) and do not  
358 accurately represent biogeochemical processes along ocean margins (Laurent et al. 2021). Model  
359 grid-spacing imposes a limit on the dynamical scales that can be explicitly resolved in the  
360 models; this is particularly problematic for coarse resolution global models because mesoscale  
361 eddies—i.e., motions on scales of about 10–100 km—dominate the variability in ocean flows  
362 (Stammer 1997). Since coarse resolution models cannot resolve mesoscale eddies explicitly, the  
363 rectified effects of these phenomena, including their role in transporting buoyancy and  
364 biogeochemical tracers, must be approximated with parameterizations (e.g., Gent and  
365 McWilliams 1990).

366 Notably, the fidelity of the simulated flow in global models, including the imperfect nature of  
367 these parameterizations, projects strongly on the model's capacity to accurately simulate  
368 ventilation and the associated uptake of transient tracers, such as anthropogenic  $\text{CO}_2$  or  
369 chlorofluorocarbons (CFCs), from the atmosphere (e.g., Long et al. 2021). Biases in the uptake of  
370 transient tracers will also have implications for a model's capacity to faithfully represent the  
371 impact of OAE, where the path of alkalinity-enhanced waters parcels in the surface ocean, and  
372 their subsequent transport to depth is a key control on the efficiency of carbon removal. Biases  
373 in the simulated flow are also an important determinant of the simulated distribution of

374 biogeochemical tracers in the model's mean state. Hinrichs et al. (2023), for example,  
 375 demonstrate that inaccuracies in the physical redistribution of alkalinity by the flow is a  
 376 dominant mechanism contributing to biases in the alkalinity distributions simulated by CMIP6  
 377 models.



378  
 379 **Figure 3:** Example of Earth System Model properties and output from the University of Victoria  
 380 Earth System Climate Model (Keller et al., 2012, Mengis et al., 2021) including a) the model  
 381 bathymetry (depth levels), and b) the simulated present-day dissolved inorganic carbon  
 382 concentration ( $\text{mol m}^{-3}$ ) averaged over the upper 50 m of the ocean. Panels c) and d) show  
 383 results from a coastal OAE study by Feng et al. (2017) where the change in upper ocean  
 384 alkalinity (upper 50 m) and the air-sea flux of  $\text{CO}_2$  are shown relative to the RCP8.5 control  
 385 simulation. Shown is the Oliv100\_Omega3.4 simulation from Feng et al. (2017), where  $100 \mu\text{m}$   
 386 olivine grains were added to ice-free coastal grid cells in proportion to RCP 8.5  $\text{CO}_2$  emissions  
 387 (i.e., 1 mol of alkalinity per mole of emitted  $\text{CO}_2$ ) until a sea surface aragonite  $\Omega$  threshold of 3.4  
 388 was reached.

389 Finally, another important challenge associated with global ocean models is the requirement to  
 390 represent the entire global ocean ecosystem with a single set of model parameters (e.g., Long et  
 391 al. 2021, Sauerland et al. 2020). In particular, the biological pump is an important control on the  
 392 distribution of biogeochemical tracers, including alkalinity and DIC. The magnitude of organic  
 393 carbon export, and the magnitude of biogenic calcium carbonate export, are important controls  
 394 on the distribution of alkalinity and DIC at the ocean surface and in the interior (e.g., Fry et al.,

395 2015). These quantities are a product of ecosystem function and, since the global ocean is  
396 characterized by diverse biogeography (e.g., Barton et al., 2013), capturing global variations in  
397 the biological pump presents a challenge.

#### 398 **2.1.4 Integration across scales**

399 Choosing the appropriate modeling tool for a given OAE-related question requires clarity about  
400 the scale of the problem to be addressed and the objectives of the model application.

401 Approaches for OAE vary significantly with respect to the spatial footprint of alkalinity  
402 increase. Proposed methods for spreading alkalinity feedstocks at the surface ocean include the  
403 addition of reactive minerals (e.g., CaO, Ca(OH)<sub>2</sub> or Mg(OH)<sub>2</sub>) in ship-propeller washes (e.g.,  
404 Köhler et al., 2013, Renforth et al., 2017, Caserini et al., 2021) or using other means (e.g., Gentile  
405 et al., 2022) along tracks from commercial or dedicated OAE vessels or through coastal outfalls  
406 (e.g., wastewater-treatment or power plants); the addition of less-reactive minerals to corrosive  
407 or high-weathering environments (e.g., olivine spreading on beaches or mineral addition to  
408 riverine discharge, e.g., Montserrat et al., 2017, Foteinis et al., 2023, Mu et al., 2023); and  
409 electrochemically generated point-sources of alkalinity that are discharged as highly alkaline  
410 seawater (e.g., House et al., 2009) from existing facilities (e.g., desalination and wastewater-  
411 treatment plants), dedicated facilities (e.g., Wang et al., 2023), or from an array of smaller  
412 infrastructure (e.g., grids of off-shore wind turbines). Models for OAE research should  
413 represent these footprints of alkalinity increases appropriately for the questions being  
414 addressed.

415 There are research questions that fall relatively neatly into one of the three scale ranges  
416 described above in sections 2.1.1 to 2.1.3. For example, consideration of the nearfield effects of  
417 different alkalinity feedstocks (e.g., dissolved versus particles) or analysis of the potential  
418 impacts from secondary CaCO<sub>3</sub> precipitation due to elevated alkalinity from a point source  
419 require models that resolve the scales of turbulent motion. Examination of the change in air-sea  
420 CO<sub>2</sub> flux due to a broad and diffuse alkalinity increase is less demanding on model resolution  
421 and regional scale models are appropriate for this question. Investigation of Earth system  
422 feedbacks requires ESMs. However, there also are many aspects of OAE that require a bridging  
423 of scales. For example, when considering different deployment methods like discharge from  
424 vessels into the ocean surface boundary layer versus additions made through outfalls via  
425 surface or subsurface plumes, modeling requirements vary. In both cases, the resulting  
426 biogeochemical response may be affected by dynamics operating in the nearfield, where  
427 conditions are sensitive to the deployment method and turbulence has to be considered, and the  
428 far-field, where conditions do not depend on the details of how the alkalinity was added and  
429 the air-sea flux of CO<sub>2</sub> is instead determined by ambient environmental processes. Another  
430 example is the challenge that anomalies in air-sea CO<sub>2</sub> flux generated by OAE deployments will  
431 manifest over large spatio-temporal scales because CO<sub>2</sub> equilibrates with the atmosphere via  
432 gas exchange slowly. Some interplay among the modeling tools described in sections 2.1.1 and  
433 2.1.2 is likely going to be required. One straightforward approach would be to parameterize  
434 small-scale processes in the larger-scale models.

## 435 2.2 The range of biogeochemical realism & complexity

436 Application of biogeochemical ocean models for the purposes of OAE research and verification  
437 requires reevaluation, and likely further development, of several model assumptions and  
438 features related to biogeochemical realism and complexity. For example, the internal sources  
439 and sinks of alkalinity are typically not explicitly represented in ocean models; this may become  
440 necessary in some circumstances but will be challenging (Section 2.2.1). OAE-related  
441 perturbations of alkalinity, other carbonate system properties, and addition of macro- and  
442 micronutrients contained in some alkalinity feedstocks may result in biological and ecosystem  
443 responses that current biogeochemical models are not capable of representing but that would be  
444 relevant for the assessment of environmental impacts of OAE and the verification its CDR  
445 efficiency (Section 2.2.2). Furthermore, depending on the environmental setting, sediments can  
446 be sources or sinks of alkalinity; these sediment-water fluxes need to be appropriately  
447 considered, including the potential impacts of OAE on their magnitude, in order to obtain  
448 complete and trustworthy carbon budgets (Section 2.2.3). Other boundary fluxes that require  
449 accurate specification are alkalinity inputs from rivers and groundwater (Section 2.2.4) and the  
450 air-sea flux of CO<sub>2</sub> across the air-sea interface (Section 2.2.5).

451

### 452 2.2.1 Representing alkalinity in seawater

453 Alkalinity is an emergent property that depends on the concentrations of numerous chemical  
454 species with distinct internal source and sinks (Schulz et al. 2023; Wolf-Gladrow et al. 2007;  
455 Middelburg et al. 2020). Skillful simulation of alkalinity in seawater may require explicit  
456 representation of its multiple biotic and abiotic sources and sinks, some of which are difficult to  
457 constrain. A major process by which alkalinity is consumed is the production of calcium  
458 carbonate. In the water column, this is predominantly a biotic process, performed by calcifiers,  
459 although “whiting” events, where calcium carbonate precipitates spontaneously from in  
460 ambient seawater can be locally important (e.g., Long et al. 2017).

461

462 Models vary in the degree of mechanistic sophistication with which biogenic calcification is  
463 represented. For example, some models explicitly resolve calcifiers, such as pelagic  
464 coccolithophores (e.g., Krumhardt et al. 2017) and foraminifera (Grigoratou et al. 2022) and, in  
465 some cases, also benthic corals, foraminifera, or calcifying higher trophic levels and thus can  
466 mechanistically account for the associated alkalinity consumption. Alternatively, models can  
467 parameterize biotic production of carbonate, and its subsequent sinking and dissolution, as a  
468 fraction of organic matter production combined with an assumed remineralization profile (e.g.,  
469 Schmittner et al. 2008; Long et al. 2021). Dissolution of carbonate minerals produces alkalinity,  
470 at the sediment surface and in the water column as carbonate particles sink. This can be  
471 represented with first-order abiotic dissolution kinetics with a dependence on the saturation  
472 state of ambient water in the water column (e.g., Sulpis et al., 2021), in the sediments (e.g.,  
473 Emerson & Archer, 1990) or in micro-environments in aggregates or organisms (Barrett et al.,  
474 2014) with systematic differences for different crystal structures, aragonite and calcite (Morse et  
475 al., 1980).

476

477 Production of alkalinity occurs via uptake of nitrate or nitrite by photoautotrophs, while  
478 remineralization consumes alkalinity when happening aerobically but generates alkalinity  
479 when occurring anaerobically, e.g. via denitrification (Fennel et al. 2008). Biotic production and  
480 consumption of alkalinity is stoichiometrically coupled to the release or uptake of nutrients and  
481 carbon, where non-Redfield processes such as nitrogen fixation or denitrification need to be  
482 specifically considered in the stoichiometric relationships (Paulmier et al., 2009).

483  
484 Spontaneous precipitation of carbonate minerals in pelagic environments could occur when  
485 seawater is highly oversaturated with respect to carbonate (Moras et al. 2022) but is, to the best  
486 of our knowledge, not yet included in ocean models. When simulating OAE approaches that  
487 may generate high oversaturation with respect to carbonate, spontaneous precipitation of  
488 carbonates needs to be considered, especially when condensation nuclei are present.  
489 Appropriate approaches will have to be developed, e.g., using near-field models to  
490 mechanistically represent this process and a meta-model approach to develop  
491 parameterizations that are suitable for far-field and larger-scale models.

492  
493 Organic compounds produced within the ocean or originating from land can also act as proton  
494 acceptors and contribute organic alkalinity (e.g., Koeve and Oschlies 2012, Ko et al. 2016,  
495 Middelburg et al. 2020) and will impact the carbonate system, the partial pressure of CO<sub>2</sub> and  
496 thus the air-sea CO<sub>2</sub> flux. Commonly, the contribution of organic alkalinity is deemed small  
497 enough in oceanic environments to be negligible, but this assumption should be reconsidered in  
498 the context of OAE, especially for coastal CDR deployments where the organic contribution to  
499 alkalinity is thought to be larger. To the best of our knowledge, models do not account for  
500 organic alkalinity. A better quantitative understanding of organic contributions to alkalinity is  
501 likely needed to parameterize or mechanistically represent its contribution in models. Similarly,  
502 it may be important in the context of mineral OAE deployments to account for local variations  
503 in [Ca<sup>2+</sup>] and [Mg<sup>2+</sup>] to accurately estimate the *p*CO<sub>2</sub> anomalies generated by different OAE  
504 feedstocks. While these constituents have very long residence times in the ocean, and are hence  
505 commonly assumed to vary conservatively in proportion to salinity, variations in their relative  
506 abundance has an impact on the thermodynamic equilibrium coefficients used to solve seawater  
507 carbonate chemistry (Hain et al., 2015).

## 508 **2.2.2 Representing biological and ecological processes**

510 A key question related to OAE is whether changes in carbonate chemistry induce differential  
511 responses in organisms. In the pelagic zone, OAE might shift the phytoplankton community  
512 composition, for example, due to distinct physiological sensitivities of different groups (e.g.,  
513 Ferderer et al. 2022). Further, if OAE is accomplished via rock dissolution, carbonate versus  
514 silicate rock may impact the relative balance between phytoplankton functional groups (PFTs)  
515 such as calcifiers and diatoms, and changes in Mg and Ca ratios may also influence calcification  
516 (Bach et al., 2019). Additionally, ancillary constituents specific to particular feedstocks may have  
517 biological activity. Silicate rocks include bioreactive metals such as Fe, a micronutrient with the  
518 capacity to stimulate phytoplankton growth, and others that are can be toxic when occurring in

519 high concentrations, such as Ni and Cu, and may adversely impact phytoplankton and reduce  
520 primary productivity (Bach et al., 2019). The bioreactivity of these metals may be difficult to  
521 simulate in models as their dissolved concentrations can be partially mediated by complexation  
522 with organic ligands (Guo et al., 2022). Physical impacts of OAE feedstocks may also have  
523 important biological impacts through changes in the propagation of light in the surface ocean,  
524 and direct exposure to mineral particles may have additional impacts, e.g., on zooplankton  
525 through particle ingestion (Harvey, 2008; Fakhraee et al., 2023). Effects of OAE on plankton  
526 have the potential to propagate to higher trophic levels through marine food webs as the  
527 magnitude and quality of net primary productivity shifts and trophic energy transfer is altered  
528 accordingly.

529  
530 Simulating this full collection of processes in models is challenging. Dominant modeling  
531 paradigms for simulating planktonic ecosystems include PFT- and trait-based models (e.g.,  
532 Negrete-Garcia et al., 2022). In these systems, physiological sensitivities are parameterized  
533 according to transfer functions that modulate rate processes—growth, for instance—on the basis  
534 of ambient environmental conditions. Nutrient limitation of growth is often represented using  
535 Michaelis–Menten kinetics wherein growth rates decline as nutrients concentrations become  
536 limiting. State-of-the-art ESMs represent PFTs with multiple nutrient co-limitation, which is  
537 essential to effectively simulate plankton biogeography of the global ocean. Diatoms, for  
538 example, are capable of high growth rates, enabling them to outcompete other phytoplankton  
539 under high-nutrient conditions, but their range is restricted to high latitudes and upwelling  
540 regions where there is sufficient silicate. If OAE were to modulate the concentration of  
541 constituents represented by multiple nutrient co-limitation models, it is possible such models  
542 could simulate the phytoplankton community response—though it’s important to consider  
543 whether the models provide representations that are sufficiently robust for the magnitude of  
544 OAE-related perturbations. In some cases, models are missing key processes that would be  
545 required to mechanistically simulate certain effects. We are aware of no models that represent  
546 Ni toxicity, for instance. Including these effects, as well as a capacity to simulate secondary  
547 interactions, such as ligand complexation of metals in OAE feedstocks, will require significant  
548 investment in empirical experimentation to understand essential rate processes and  
549 physiological responses.

550  
551 Shortcomings in the capacity of models to represent physiological responses to OAE is an  
552 important consideration for the ability of models to faithfully represent ecological impacts.  
553 Notably, electrochemical OAE techniques present a simpler set of processes to consider than  
554 using crushed-rock feedstocks, where ancillary constituents and physical dynamics come into  
555 play. For electrochemical OAE, the most likely biological feedback to consider relates to the  
556 impacts of changing carbonate chemistry on biogenic rates of calcification or phytoplankton  
557 growth rates (Paul and Bach 2020). It is also possible that carbon limitation of phytoplankton  
558 growth (Paul and Bach 2020; Riebesell et al. 1993) may also be important. Empirical research  
559 exploring physiological sensitivities should be used to develop prioritizations of key model  
560 processes comprising early targets for implementation. Model documentations should use  
561 consistent stoichiometric relations to link alkalinity changes to those of nutrients and carbon

562 (Paulmier et al. 2009) and state the assumptions made about carbonate formation and  
563 dissolution.

564

### 565 **2.2.3 Representing sediment-water exchanges**

566 The exchange of solutes between the sediments and overlying water influences ocean  
567 chemistry, including the properties of the carbonate system (Burdige 2007). Depending on  
568 location and time scale, OAE may affect these exchanges and should be appropriately  
569 considered in models. Sediments influence the marine carbonate system primarily through the  
570 remineralization of organic matter, which returns DIC to overlying water (and alkalinity if this  
571 remineralization occurs anaerobically), and the dissolution of biogenic silicate or carbonate  
572 minerals.  $\text{CaCO}_3$  is of particular importance as its dissolution releases alkalinity, while its burial  
573 is an alkalinity sink, and the balance between the two is a key control on the ocean's alkalinity  
574 balance over timescales approaching  $10^4$  years (Middelburg et al. 2020). Furthermore,  
575 remineralization and other microbial metabolisms, such as "cable bacteria," can significantly  
576 lower pore water pH by several pH units below seawater values (Meysman and Montserrat  
577 2017). This can drive dissolution of  $\text{CaCO}_3$  and generate alkalinity in the sediments, even in  
578 shallow waters when the overlying water is supersaturated (Rau et al. 2012).

579

580 Representing these processes in coastal and shelf sediments (< 200 m) is challenging. Shallow  
581 water depths and high productivity result in a significant delivery of organic matter to the  
582 sediments that is much larger than in the deep ocean. As a result, the relative importance of  
583 sediments in organic matter remineralization is larger and production of alkalinity by anaerobic  
584 metabolisms is more important in these shallow sediments than in the deep ocean (Seitzinger et  
585 al. 2006, Jahnke 2010, Huettel et al. 2014, Chua et al. 2022). In addition, these environments are  
586 dynamic with organic supply and bottom water conditions varying on tidal, seasonal, and  
587 interannual timescales. Accounting for the exchange between sediments and overlying water  
588 and its variability on tidal, seasonal, and interannual timescales will likely be necessary in  
589 regional and global biogeochemical models that aim to simulate alkalinity cycling in coastal and  
590 shelf seas, even for relatively short simulation durations of months to years.

591

592 The choice of approach to modeling sediments may depend on the sediment type. For example,  
593 the mechanisms transporting solutes across the sediment-water interface can be divided into  
594 two categories depending on the sediment's grain size. In coarse sediments, i.e. permeable  
595 sands, pressure gradients drive flow through the seabed replenishing sediment oxygen content  
596 (Huettel et al. 2014). Organic carbon stores are low and remineralization was long thought to be  
597 primarily aerobic. However, evidence has emerged relatively recently that anaerobic  
598 remineralization in sandy sediments is more important than originally thought (Chua et al. 2022  
599 and references therein). Idealized models that represent the three-dimensional sediment  
600 structure illustrate the importance of turbulence and oscillatory flows in permeable sediments  
601 (see Box 2 in Chua et al. 2022). These models are highly localized and computationally  
602 demanding, prohibiting their coupling with ocean biogeochemical models. Thus, permeable



603 sediments are currently not well represented in regional or global ocean biogeochemical  
604 models.

605  
606 In cohesive, fine-grained sediments with low permeability, i.e. muds, transport is limited by  
607 diffusion or faunal mediated mixing and exchange processes, i.e. bioirrigation or bioturbation  
608 (Meysman, et al. 2006, Aller 2001). In these environments, detailed multicomponent reactive-  
609 transport models of sediment biogeochemistry – so called diagenetic models – can reproduce  
610 carbon remineralization rates partitioned between aerobic and anaerobic pathways,  
611 precipitation/dissolution reactions between sediment grains and porewaters, and the transport  
612 of solutes across the sediment-water interface (Boudreau 1997, Middelburg et al., 2020). These  
613 mechanistic models will be useful for detailed investigations into how perturbations of the  
614 carbonate system in seawater overlying the sediments affect their biogeochemistry and for  
615 addressing questions about the potential influence of particulate alkalinity feedstocks settling to  
616 the seafloor (Montserrat et al. 2017, Meysman and Montserrat 2017). However, typically these  
617 models are one-dimensional and applied to a few representative locations. Coupling fully  
618 explicit diagenetic models to three-dimensional ocean biogeochemical models, while  
619 conceptually straightforward, is computationally prohibitive. Instead, depth-integrated  
620 sediment processes have been implemented as bottom boundary conditions (e.g., Moriarty et al.  
621 2017, 2018, Laurent et al. 2016). For example, Laurent et al. (2016) used a diagenetic model in a  
622 “meta-modeling” approach to estimate bottom boundary nutrient fluxes for a regional scale  
623 biogeochemical model. By parameterizing the diagenetic model with detailed geochemical data  
624 (porewater profiles and nutrient fluxes) from a few individual locations, then forcing it over a  
625 range of expected bottom water conditions, they developed empirical functions relating  
626 sediment fluxes to bottom water conditions that could be used to parameterize bottom  
627 boundary conditions in the water column model. A similar approach could be used in OAE  
628 models to parameterize how sediment biogeochemistry may alter alkalinity fluxes, for example,  
629 how redox sensitive processes, such as coupled nitrification-denitrification or sulfate reduction  
630 coupled to pyrite burial, both of which may produce alkalinity (Soetaert et al. 2007), may  
631 respond to changes in bottom water oxygen or organic matter loading.

632  
633 When considering the long-term storage of CO<sub>2</sub> in global-scale ESMs, the interactions between  
634 sediments and the deep ocean (> 1000 m bottom depth) may need to be considered. In this  
635 environment most organic matter remineralization occurs in the water column, and the small  
636 amount of organic matter reaching the seafloor is remineralized aerobically with little to no  
637 release of alkalinity. In this case, sediment remineralization can likely be either ignored or  
638 implemented as a reflective boundary condition where the simulated POC flux to the seafloor is  
639 immediately returned as DIC and remineralized nutrients. However, the dissolution or  
640 preservation of CaCO<sub>3</sub> in deep sediments is critical to controlling deep water alkalinity and may  
641 be important in model simulations that aim to quantify OAE effects on the timescales associated  
642 with the large-scale global overturning circulation. CaCO<sub>3</sub> solubility increases with pressure  
643 and decreasing pH and CaCO<sub>3</sub> eventually becomes undersaturated at depth. The depth at  
644 which sinking CaCO<sub>3</sub> balances its dissolution is referred to as the carbonate compensation  
645 depth (CCD). An increase in bottom water CO<sub>3</sub><sup>2-</sup> or CaCO<sub>3</sub> deposition, will deepen the CCD,

646 burying  $\text{CaCO}_3$ , trapping alkalinity, and lowering the alkalinity budget of the ocean.  
647 Conversely if  $\text{CaCO}_3$  rain rate or  $\text{CO}_3^{2-}$  concentration decreases, the CCD will shoal and  
648 previously buried  $\text{CaCO}_3$  will dissolve releasing alkalinity to the deep ocean. CCD  
649 compensation therefore opposes any forcing of the deep ocean carbonate system and therefore  
650 dampens the rise of  $\text{CO}_2$  in the atmosphere but will also counteract any potential OAE solution  
651 (see Renforth and Henderson 2017 for a detailed explanation). Although most  $\text{CaCO}_3$   
652 dissolution occurs in the sediments, there is no consensus as to the level of detail this needs to  
653 be represented in models. Some global models employed to investigate large-scale OAE include  
654 calcium carbonate dynamics at the sediment surface (Ilyina et al. 2013) others disregard this  
655 process (Keller et al. 2014).

656  
657 Often global models will parameterize  $\text{CaCO}_3$  burial as a function of saturation state, such an  
658 approach is effective for resolving CCD dynamics over geological timescales ( $\sim 10,000$  y), but not  
659 over the century to millennial timescales of CCD readjustment. Models that fully couple  
660 sediment diagenesis can resolve these dynamics (Gehlen et al. 2008), but the computational  
661 demand can make them ineffective. One solution is the approach of Boudreau et al. (2010) and  
662 (2018). By suggesting that  $\text{CaCO}_3$  dissolution dynamics are controlled by transport of  
663 dissolution products across the benthic boundary layer, they were able to derive equations  
664 predicting CCD depth and  $\text{CaCO}_3$  dissolution based on bottom water  $\text{CO}_3^{2-}$  and  $\text{CaCO}_3$  rain rate  
665 and avoiding a detailed representation of the sediments. These equations, combined with model  
666 bathymetry, can parameterize sediment  $\text{CO}_3^{2-}$  flux as a boundary condition and suitably account  
667 for transient sediment  $\text{CaCO}_3$  dissolution in large scale ESMs while avoiding the computational  
668 demands of a fully coupled ocean circulation-diagenesis model.

#### 669 *2.2.4 Representing river and groundwater fluxes*

671 Regional and global ocean biogeochemical models typically account for river inputs, including  
672 their contributions to alkalinity and DIC. In most models this is done by specifying alkalinity  
673 and DIC concentrations in imposed riverine freshwater fluxes, although accurate prescription of  
674 these concentrations can be challenging. Typically, a combination of direct river measurements,  
675 where available, output from watershed models (e.g., Seitzinger et al. 2010), or extrapolations of  
676 coastal ocean measurements to a freshwater endmember (e.g., Rutherford et al. 2021) are used.  
677 Solute inputs from groundwater are typically ignored but could be important locally. In high-  
678 resolution coastal domains near urban areas, sewage input may be an additional important  
679 source of carbon, nutrients, and alkalinity.

680  
681 It is important to note that land-based CDR applications may have an important effect on ocean  
682 alkalinity dynamics through riverine and groundwater delivery of solutes. Terrestrial OAE  
683 equivalents broadly referred to as Enhanced Rock Weathering (ERW) rely on the application of  
684 lime or pulverized silicate or carbonate rocks on land and in rivers. These strategies aim to  
685 generate  $\text{CO}_2$  uptake locally but yield a leaching flux of bicarbonate into freshwater systems and  
686 subsequent transport into the coastal ocean. Field trials and some commercial applications are  
687 currently underway, most of them with the implicit or explicit assumption that the enhanced

688 delivery of alkalinity will generate a carbon removal in the ocean (Köhler et al., 2010; Taylor et  
689 al., 2016; Bach et al., 2019). There is a need for coordinated efforts to improve quantification of  
690 background riverine fluxes and establish initiatives to effectively track the solute additions from  
691 ERW.

692

### 693 2.2.5 Representing air-sea gas exchange

694 The calculation of air-sea gas exchange is necessary for the quantification of net carbon uptake  
695 from OAE in models. Biogeochemical models typically represent this exchange using a bulk  
696 relationship that depends on the product of the gas transfer velocity and the effective air-sea  
697 concentration difference (Fairall et al. 2000). However, the gas transfer velocity remains highly  
698 uncertain and is sensitive to a collection of processes that vary across scales, including sea state,  
699 boundary layer turbulence, bubble dynamics, and concentrations of surfactants. The most  
700 widely used parameterizations of the gas transfer velocity use empirical fits to observations to  
701 construct a functional relation dependent on wind speed only, under the premise that  
702 turbulence and bubbles (via the breaking of surface gravity waves) are predominantly  
703 determined by wind stress (Wanninkhof 2014). This neglects processes that could be regionally  
704 important such as convection, modification by biological surfactants, rain and wave-current  
705 interactions, while vastly simplifying the effects of wave breaking and bubbles. Although  
706 different dependencies on wind speed have been proposed (quadratic, cubic, hybrid),  
707 parameterizing the gas transfer coefficient as a quadratic function of the 10-meter wind speed is  
708 the most common (Wanninkhof 1992; Wanninkhof 2014). This relationship is supported by  
709 direct measurements of air-sea flux at intermediate wind speeds (3-15 m/s), but at low wind  
710 speeds (< 3 m/s), non-wind effects can have an important impact on gas transfer. At high wind  
711 speeds (> 15 m/s), breaking waves and bubble injection enhance gas exchange for lower  
712 solubility gasses such as CO<sub>2</sub> (Bell et al. 2017). Therefore, quadratic fits tend to underestimate  
713 the gas exchange at low and high wind speeds (Bell et al. 2017).

714

715 More complex air-sea exchange parameterizations account for processes such as bubbles, near  
716 surface gradients and buoyancy driven convection (e.g., Liang et al. 2013, Fairall et al. 2000), but  
717 they depend upon a wider range of input variables. Other considerations in estimating flux  
718 arise from the nonlinear dependence on these variables, e.g., wind speed, which can lead to  
719 underestimates when made using daily averages rather than hourly measurements (Bates and  
720 Merlivat 2001).

721

722 Notably, the gas transfer velocity ( $k_w$ ) determines the kinetics of gas exchange, given a  
723 perturbation in surface ocean  $p\text{CO}_2$  away from equilibrium. The timescale for CO<sub>2</sub> equilibration  
724 over the surface mixed layer can be fully quantified using the following expression,

$$725 \tau_{gas-ex} = \left( \frac{\partial \text{CO}_2}{\partial \text{DIC}} \right)^{-1} \left( \frac{h}{k_w} \right)$$

726 where  $h$  is the depth of the surface mixed layer and the partial derivative  $\partial \text{CO}_2 / \partial \text{DIC}$  captures  
727 the thermodynamic state of the carbon system chemistry in seawater, specifically with respect  
728 to the amount that dissolved CO<sub>2</sub> changes per unit change in DIC (Sarmiento and Gruber 2006).

729 This property is related to the buffer capacity and varies in roughly linear proportion to the

730 carbonate ion concentration. The magnitude of  $\left(\frac{\partial CO_2}{\partial DIC}\right)^{-1}$  is typically about 20, which explains  
731 why the equilibration timescale for CO<sub>2</sub> is so long. The contribution of uncertainty in the gas  
732 exchange velocity to overall uncertainty in carbon uptake from OAE deployments will depend  
733 in part on the circulation regime involved. For example, in situations where alkalinity-enhanced  
734 water parcels are retained at the surface for timescales that are significantly longer than  $\tau_{\text{gas-ex}}$ ,  
735 full equilibration will occur and the impact of uncertainty in the gas exchange velocity will have  
736 limited influence on the overall uncertainty.

737  
738 Even though OAE-induced additional air-sea CO<sub>2</sub> fluxes will, even in hypothetical massive  
739 deployments, amount to at most a few Gt CO<sub>2</sub>/yr, which is typically not more than a percent of  
740 the atmospheric CO<sub>2</sub> inventory, this subtle difference in the treatment of the atmospheric  
741 boundary condition can be significant. Using prescribed atmospheric  $p\text{CO}_2$  that is unresponsive  
742 to marine CDR-induced air-sea CO<sub>2</sub> fluxes has been shown to overestimate oceanic CO<sub>2</sub> uptake  
743 by 2%, 25%, 100% and more than 500% on annual, decadal, centennial, and millennial  
744 timescales, respectively (Oschlies 2009). Simulations with prescribed atmospheric  $p\text{CO}_2$  need to  
745 take such systematic biases into account.

### 746 **2.3 Model development needs for OAE research**

748 While there is already substantial capacity for simulating ocean biogeochemical dynamics at  
749 global to regional scales, the discussion above implicates several areas where additional efforts  
750 are required to fully establish a modeling capability suitable for supporting OAE. These fall into  
751 four primary areas: (1) supporting multi-scale simulations with sufficiently high-fidelity flow  
752 fields; (2) faithfully simulating the near-field dynamics associated with alkalinity addition; (3)  
753 capturing feedbacks to OAE owing to biological and geochemical responses; and (4) identifying  
754 whether there are reduced-complexity modeling approaches that might provide sufficiently  
755 robust estimates of the net effects of OAE.

756 As elucidated above, a primary consideration related to capturing OAE impacts is the fidelity of  
757 the simulated flow. Notably, OAE presents a somewhat novel use case requiring an effective  
758 multi-scale modeling capability. A conceptually straightforward path to improving the  
759 representation of ocean circulation and mixing is to increase the resolution of the model grid.  
760 However, the computational demand of high-resolution simulations can only be met over more  
761 limited-area domains. Since the spatiotemporal footprint of OAE-related perturbations is likely  
762 to be large, there will be a need to represent large regions. An argument might be made,  
763 however, that the circulation in proximity of an OAE site is most important to capture with  
764 high-fidelity. This can be achieved with two-way nested regional models as described in see  
765 Section 2.1.2 but will require further development to couple in the nearfield models described in  
766 Section 2.1.1. Native grid-refinement, e.g. via unstructured grids, is another approach that may  
767 be pursued to effectively support OAE research.

768 The second area of model development relates to the requirement of faithfully representing the  
769 dynamics associated with alkalinity addition. Regional to global scales are the most relevant for  
770 simulating the air-to-sea exchange of CO<sub>2</sub> ensuing from OAE. It is important, however, to

771 ensure that local processes affecting the mass fluxes and initial dispersal of alkalinity are  
772 handled appropriately. As illustrated above, DNS or LES simulations (section 2.1.1) can be  
773 leveraged to develop parameterizations for larger-scale models, including for crushed-rock  
774 feedstocks where particle dynamics may be important or techniques involving alkalinity  
775 enhanced streams entering the ocean from outfall pipes. In addition to process fidelity, there are  
776 also numerical constraints to consider. For example, advection schemes used in most ocean  
777 general circulation models struggle to represent sharp gradients; large mass fluxes of alkalinity  
778 into single model grid-points are likely to cause advection errors that may contaminate aspects  
779 of the model solutions making interpretation difficult. More specifically, conservative advection  
780 schemes can be characterized in terms of their accuracy, monotonicity (i.e., ability to preserve  
781 sign), and linearity (i.e., ability to preserve additivity) and there are always tradeoffs to make  
782 between these properties. Research may be required to determine which schemes are best  
783 suited to the particular challenges associated with representing the advection of OAE signals.

784 The third area of model development relates to our capacity to fully capture the range of  
785 biogeochemical feedback associated with OAE. The class of processes to consider here is  
786 potentially large and many have been touched on in section 2.2.1 to 2.2.3. Precipitation  
787 dynamics, specific elemental components of alkalinity, biogenic responses mediated by  
788 physiological or ecological sensitivities, impacts and processes controlling the cycling of  
789 ancillary constituents, and accurate sediment-water exchange are all areas that merit  
790 consideration. Further efforts are required to understand and prioritize these areas of potential  
791 development and, notably, their relative importance is likely to be regionally dependent.

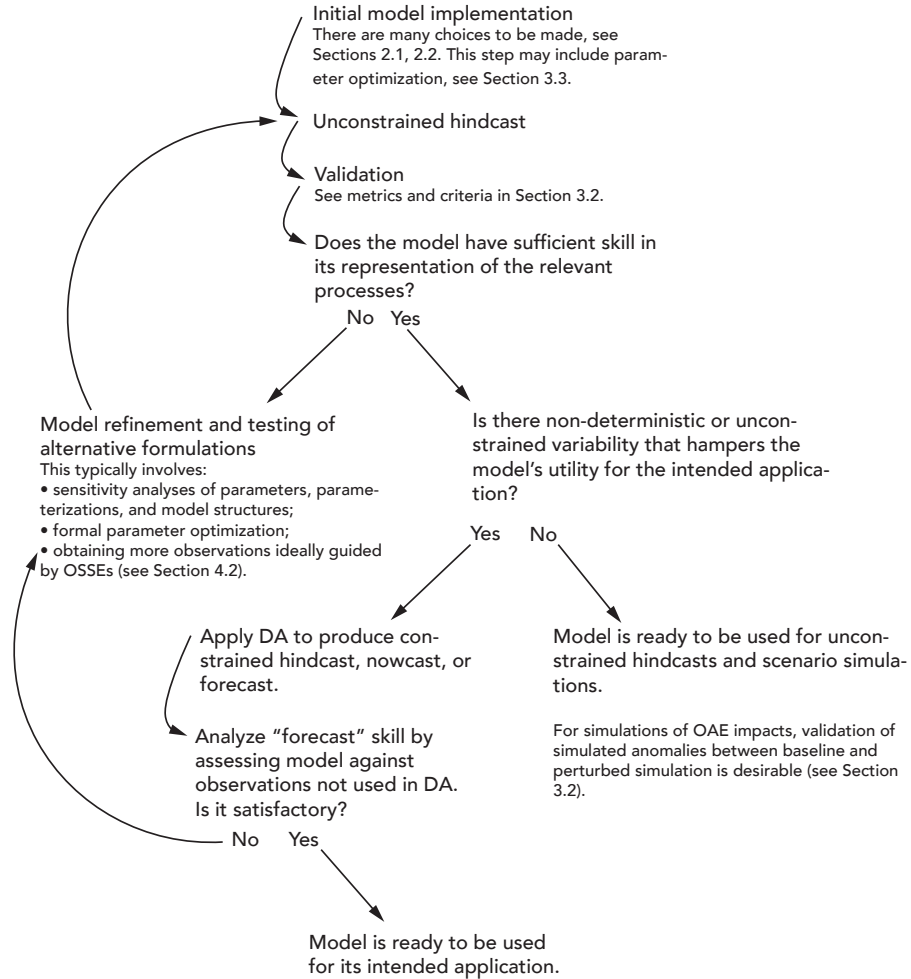
792 Finally, it is important that models be tailored to address specific questions of relevance. In this  
793 context, it may be important to consider how much model complexity is required to capture the  
794 effects of perturbations, seeking parsimonious representations that are well-supported by  
795 empirical constraints and invoking wherever possible a separation of concerns to isolate the  
796 factors contributing to uncertainty. For example, there are several near-field considerations that  
797 might be addressed using a combination of local observations and ultra-high-resolution  
798 modeling tools to generate estimates of alkalinity mass fluxes that are subsequently imposed as  
799 forcing in regional- to global-scale models. Another key question is how important it is to  
800 comprehensively simulate the mean state to faithfully capture the response to OAE  
801 perturbations for the purpose of MRV. For example, if it can be documented that biological  
802 feedbacks to OAE are of negligible concern, the core target for simulating OAE effects for MRV  
803 may be to capture the cumulative integral of air-sea CO<sub>2</sub> exchange associated with the induced  
804 surface ocean *p*CO<sub>2</sub> anomaly. The mean state of the seawater carbon system is relevant here as  
805 the background DIC and alkalinity fields determine the *p*CO<sub>2</sub> response per unit addition of  
806 alkalinity, but fully prognostic calculations of nutrient cycling may not be necessary.

### 807 **3 Model validation and integration with observations**

808 Whether a model is useful for OAE research depends on how accurately it represents the  
809 physical, chemical, and biological processes that are relevant to the specific research question to  
810 be addressed. Model validation, the evaluation of a model's performance, and estimation of

811 uncertainties in model output should thus be integral parts of model implementation and  
 812 application. It is important to note that any model, even after best efforts have been made to  
 813 improve formulations and conduct the most thorough validation, will deviate from reality. Any  
 814 model is, by definition, a simplification of the real world and thus its output will be subject to  
 815 uncertainties. Deviations of the model state from the real world can be reduced by applying  
 816 statistical techniques, collectively referred to as Data Assimilation (DA) methods, that combine  
 817 models with observations and yield the best possible estimates. The steps typically involved in  
 818 model implementation and validation, and possible integration with observations through data  
 819 assimilation are shown in Figure 4. In this section, we summarize the most important  
 820 observation needs for model validation (Section 3.1), briefly describe typical metrics for model  
 821 validation and articulate a reasonable minimum criterion (Section 3.2), give a high-level  
 822 explanation of approaches for the formal statistical combination of models with observations  
 823 through parameter optimization and state estimation (Section 3.3), and describe approaches for  
 824 the specification of uncertainty in model outputs (Section 3.4).

825



826

827

828 **Figure 4:** Typical steps in model implementation and validation.

### 829 3.1 Observation types for validation

830 Two fundamental requirements for models to be useful in the context of OAE research are high-  
831 fidelity representations of physical transport due to advection and mixing, and of  
832 biogeochemical effects of OAE, most importantly changes in the inorganic carbon properties.

833 Observations for validation of the simulated physical transport of alkalized waters include  
834 temperature and salinity distributions, direct measurements of currents, surface drifter  
835 trajectories, sea surface height observations from satellite altimetry, and estimates of  
836 geostrophic flow derived from the latter. Additional metrics relevant for assessing the fidelity of  
837 the large-scale overturning circulation in global models include combinations of biogeochemical  
838 concentration and transient tracers. For example, oxygen can be useful for identifying large-  
839 scale transport pathways, even though it convolutes dynamical and biological information.  
840 Particularly valuable for assessing large-scale ocean transport on the timescales relevant for  
841 OAE are abiotic transient tracers such as such as chlorofluorocarbons (CFCs), sulfur  
842 hexafluoride (SF<sub>6</sub>), and possibly the isotopes <sup>39</sup>Ar and <sup>14</sup>C. Observational approaches for  
843 validation at regional scales include explicit tracer studies for documenting dispersion  
844 properties using Rhodamine dye or SF<sub>6</sub>.

845 In addition to the dynamics of the flow, model validation for OAE research requires the  
846 assessment of the fidelity of simulated carbonate chemistry variables (e.g., alkalinity, total  
847 dissolved inorganic carbon or DIC, pH, *p*CO<sub>2</sub>) and salinity and temperature, which are used to  
848 calculate the 13 thermodynamic equilibrium constants and conservative chemical species  
849 needed to constrain seawater acid-base chemistry in oxygenated seawater. Depending on the  
850 OAE approach and the model application, assessment may also require observed macronutrient  
851 (e.g., nitrate, silicate, or phosphate), micronutrient (e.g., Fe), and contaminant (e.g., Ni, and Cr)  
852 measurements; bulk seawater properties related to biogeochemical cycling (e.g., dissolved  
853 organic carbon content [DOC], particulate inorganic carbon [PIC], chlorophyll fluorescence);  
854 and biogeochemical rates and fluxes (e.g., net community calcification).

855 It is not always feasible to obtain the ideal carbonate system observations for model validation.  
856 Temperature and salinity can be measured reliably across all ocean depths and, with greater  
857 uncertainty and only at the ocean surface, remotely from satellites. The technical capacity for  
858 seawater pH measurements is evolving rapidly and sensors and systems now exist for pH  
859 measurements across nearly all depths, though the depth-capable systems require regular  
860 recalibration (e.g., Maurer et al., 2021). Similarly, there are numerous ways to observe surface  
861 ocean *p*CO<sub>2</sub> using a variety of crewed, autonomous, and fixed-location platforms (e.g., ship-  
862 based, Saildrone, and moored systems). However, interior-ocean *p*CO<sub>2</sub> observations remain  
863 challenging to obtain due to the need for calibration gasses and a gas-water interface. Alkalinity  
864 titrations are predominantly performed on discrete bottle samples collected by hand, though  
865 autonomous titration systems are under development that enable *in situ* surface time series  
866 measurements (Shangguan et al., 2022). Microfluidic *in situ* alkalinity titrators are also under  
867 development that consume less reagent per sample but currently show higher uncertainties  
868 than discrete samples (Sonnichsen et al. 2023). Solid state titrators that generate acid titrant *in*

869 *situ* show promise for surface and subsurface alkalinity titrations, but these sensors are still  
870 undergoing development and validation (Briggs et al., 2017). DIC observations combine the  
871 limitations of current measurement systems for both the  $p\text{CO}_2$  and alkalinity, and there are only  
872 a handful of automated DIC titration systems rated for surface ocean measurements (e.g.,  
873 Fassbender et al. 2015; Wang et al. 2015; Ringham 2022). Theoretically, measurement of two of  
874 the carbonate system parameters in combination with temperature and salinity and some  
875 additional assumptions allows calculation of the other carbonate system parameters in  
876 seawater. Unfortunately, the pair of  $p\text{CO}_2$  and pH, which are the most accessible to autonomous  
877 measurement among the carbonate system parameters, provide nearly identical information  
878 about the system. Thus, the results of the calculations that use this pair have higher  
879 uncertainties than other combinations (Dickson and Riley 1979; Millero 2007; Cullison Gray et  
880 al. 2011; McLaughlin et al. 2015; Raimondi et al. 2019) and are therefore not ideal as a pair for  
881 model validation.

### 882 3.2 Validation metrics and approach

883 Validation relies on comparing the model output to observations, often in an iterative loop  
884 where the evaluation of a hindcast simulation is followed by model refinements followed in  
885 turn by a new hindcast and re-evaluation (Figure 4, Rothstein et al. 2006). Several evaluation  
886 metrics are commonly used (see Box 3 in Fennel et al. 2022). The three most common are the  
887 root-mean-square error (RMSE), the bias, and the correlation coefficient. All three are relative  
888 measures without any objective criterion that indicates which range of values is acceptable or  
889 unacceptable. In contrast, the Z-scores, which consider variability within the observational data  
890 set, and the so-called model efficiency or model skill, which quantifies whether the model  
891 outperforms an observational climatology are two metrics with built-in criteria as to whether a  
892 model's performance is acceptable or not (Fennel et al. 2022). Since no single metric provides a  
893 complete picture of a model's skill, multiple complementary metrics should always be used in  
894 combination (Stow et al. 2009). Furthermore, different points in space and time, and a breadth of  
895 variable types should be part of any comprehensive validation because a model may provide  
896 accurate estimates for some variables, locations, or times but perform poorly for others (Doney  
897 et al. 2009).

898 For OAE research, validation can be considered as a two-step challenge. First, it is necessary to  
899 validate unperturbed model baselines to gain confidence that the natural variability is  
900 represented appropriately and to quantify model uncertainties. One should compare model-  
901 simulated spatial fields and time-series at strategic locations with appropriate observations to  
902 assess the model's skill at representing mean distributions as well as the variability for  
903 carbonate chemistry measurements and other relevant properties using several of the  
904 complementary quantitative metrics listed above. A model could be considered as sufficiently  
905 validated when mean distributions, their seasonal variability, and the timing and magnitude of  
906 events (e.g., blooms, physical disturbances) are accurately represented. As described in Section  
907 3.1, insufficient availability of observational constraints on carbonate system parameters  
908 presents a major challenge in this regard. In models applied for OAE research, it is particularly  
909 important to assess whether they realistically capture the distributions and variability of



910 seawater properties that govern sensitivity of the seawater carbonate system; recent work by  
911 Hinrichs et al. (2023) shows that the current representation of alkalinity in state-of-the-art  
912 models requires improvements.

913 The second, even more difficult step is to test whether a model accurately represents alkalinity  
914 additions. OAE-related modeling studies thus far have relied on models that are validated only  
915 for baseline conditions. These are useful as sensitivity studies. However, validation of a model's  
916 ability to accurately represent the perturbations of an alkalinity addition is ultimately needed to  
917 address OAE science questions around environmental impacts and MRV. It is likely that the  
918 metrics described above for baseline validation are not suitable for this task. Validation should  
919 focus on quantifying whether the model accurately captures the anomalies created by OAE.  
920 This requires consideration of the spatial footprint and temporal evolution of perturbations and  
921 ideally a close integration of experimental, observational, and modeling efforts. For example, a  
922 model that is deemed skillful after baseline validation can be used to estimate the appropriate  
923 dosage of alkalinity additions, thus ensuring a measurable signal, and guide the observational  
924 strategy; subsequent validation may indicate model shortcomings that were not obvious in the  
925 baseline validation (e.g., diverging dissipation rates between model and field observations) and  
926 prompt model refinement in an iterative loop of model validation, improvement, and renewed  
927 experimental assessment (Figure 4).

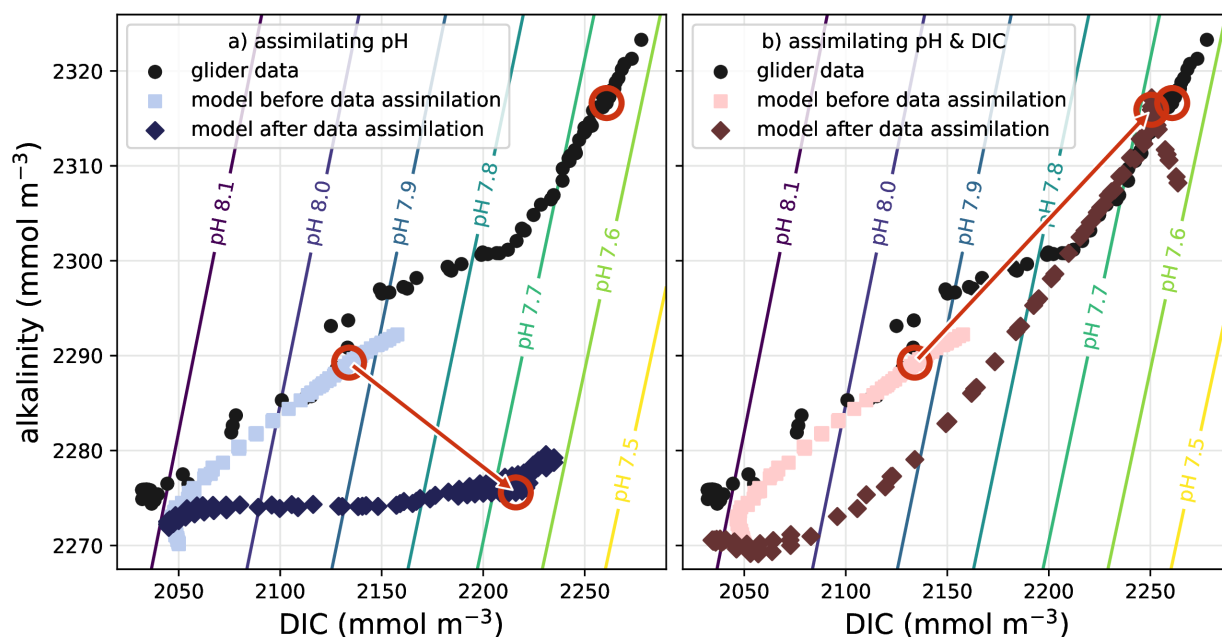
928 It is important to note that even with repeated steps of validation and model improvement,  
929 there is going to be a limit to the degree of realism that can be achieved with any model. Any  
930 model simulation will be prone to errors and uncertainties. Sources of error include inaccuracies  
931 in model inputs, numerical approximation schemes, insufficient process understanding, and  
932 inaccurate model parameters and parameterizations.

### 933 **3.3 Data Assimilation**

934 Data assimilation (DA) is the process of improving the dynamical behavior of models by  
935 statistically combining them with observations. There are a variety of DA techniques that rely  
936 on different mathematical and statistical approaches (Carrassi et al. 2018). Originally developed  
937 for numerical weather prediction, DA has been successfully applied to ocean models, including  
938 biogeochemical models (Mattern et al. 2017, Cossarini et al. 2019, Ciavatta et al. 2018, Verdy and  
939 Mazloff 2017, Teruzzi et al. 2018, Fennel et al. 2019) but success critically depends on the  
940 information content of the available observations (Yu et al. 2018; Wang et al. 2020). While DA  
941 has been shown to yield large improvements in important parameters governing  
942 biogeochemical processes (Mattern et al. 2012, Schartau et al. 2017, Wang et al. 2020) and in  
943 model estimates of the physical and biogeochemical model state (Hu et al. 2012, Mattern et al.  
944 2017, Ciavatta et al. 2018), it is only starting to be applied to carbonate system properties (Verdy  
945 and Mazloff 2017, Carroll et al. 2020, Turner et al. 2023, Figure 5).

946 Application of DA for ocean models is typically applied for one of two purposes: (1) to  
947 systematically optimize model parameters, e.g., phytoplankton growth and nutrient uptake or  
948 rates of background dispersion, and (2) to estimate the ocean state, e.g., distributions of  
949 temperature, phytoplankton biomass, alkalinity (see Fennel et al. 2022 for more details on the

950 practical approaches and examples). The first purpose addresses systematic errors and biases in  
 951 models and is useful when systematically modifying and testing different model formulations  
 952 while the second assumes an unbiased model and addresses unresolved stochasticity, e.g.,  
 953 correcting the locations of mesoscale eddies and current meanders. State estimation offers the  
 954 potential to constrain variability such that OAE-induced perturbations of carbonate system  
 955 parameters can be documented even if they are smaller than the natural variability in the study  
 956 region. Joint estimation of physical and biogeochemical properties is common and can yield  
 957 significant improvements for both types of properties (Yu et al. 2018). Hybrid approaches  
 958 combining parameter and state estimation have also been proposed (Kitagawa 1998, Mattern et  
 959 al. 2012, 2014) but are less widely used.



960  
 961 **Figure 5:** Example of a DA application for state estimation of carbonate system properties  
 962 within a 3-dimensional model of the California Current System. The symbols show glider data  
 963 and model estimates at the measurement times and locations; one specific data point and its  
 964 associated model estimates are highlighted by red circles. Each data point consists of measured  
 965 pH alongside estimated alkalinity and DIC values (see Takeshita et al. (2021) for data source  
 966 and details). In the model, pH is a diagnostic variable and primarily dependent on the model's  
 967 alkalinity and DIC estimates. (a) When only pH data is assimilated, the model estimates are  
 968 moved closer to the observed pH values by increments in alkalinity-DIC space that degrade the  
 969 model's alkalinity estimates. (b) The model state estimates improve considerably by  
 970 assimilating data for DIC (or alkalinity; not shown) together with the pH observations.

971 Successful application of DA critically requires sufficient observations either of the properties  
 972 that the model parameters to be estimated depend on or of the state variables that are being  
 973 estimated. The most commonly used observation type in biogeochemical DA applications is  
 974 satellite-based ocean color observations (Mattern et al. 2017, Ciavatta et al. 2018, Teruzzi et al.  
 975 2018) which are available at a relatively high temporal resolution and covering large areas of the

976 surface ocean. While these observations are useful for informing model estimates of properties  
977 directly linked to processes involving phytoplankton, they provide little information on the  
978 carbonate system. Dynamical models are able to quantitatively constrain processes that cannot  
979 be measured directly, by inferring them from observable properties, but only if the observations  
980 contain enough relevant information about the processes of interest. Hence, one of the biggest  
981 challenges facing the application of DA to models of the marine carbonate system, is the  
982 sparsity of observations of the marine carbonate system. Observations of pH, pCO<sub>2</sub>, alkalinity,  
983 and DIC used to be limited to moorings and research cruises but have more recently been  
984 extended by automated observing systems, such as gliders, BGC-Argo floats and uncrewed  
985 surface vehicles (Bushinski et al. 2019). Although these measurements are becoming more  
986 common (Chai et al. 2020), they are still sparse compared to what is typically required for DA  
987 applications. In this context, an additional challenge is the problem of underdetermination, i.e.  
988 if multiple processes or properties of interest can cause a similar change in an observable  
989 property, then observing this property alone may not hold enough information to constrain  
990 these processes or properties and more observations are needed (see Figure 5 and code  
991 examples in Fennel et al. 2022). As new platforms are added to the observing system, DA  
992 techniques can help guide their optimal deployment and tailor observational programs to the  
993 specific needs of OAE applications (see Section 4.3 below). Furthermore, statistical and  
994 machine-learning approaches are being developed (e.g., Lohrenz et al. 2018, Bittig et al. 2018, in  
995 prep.) that may help overcome the undersampling of carbonate system properties and could  
996 feed directly into DA applications.

997 There is an important subtlety to the application of data-assimilative models when quantifying  
998 net CO<sub>2</sub> uptake due to OAE, which is highly relevant for MRV. When the net CO<sub>2</sub> uptake is  
999 quantified by calculating the difference between two simulations, one with and one without  
1000 OAE (one of these is realistic, the other counterfactual), it is not appropriate to assimilate  
1001 biogeochemical observations of properties affected by the alkalinity enhancement. The  
1002 assimilation of alkalinity-related observations to constrain one of the simulations in the pair  
1003 would eliminate the ability to make comparisons between the two. However, assimilation of  
1004 observations that are unaffected by OAE (e.g., temperature, salinity, oxygen, etc.) can be  
1005 applied to both simulations of the pair. Further research and method development are required  
1006 to identify the best approaches for leverage DA in this context.

### 1007 1008 **3.4 Uncertainty analysis**

1009 Model results should be paired with sound qualitative and quantitative uncertainty estimates,  
1010 especially when used for practical decisions. Estimating the uncertainty of model simulations,  
1011 however, is inherently difficult because typically one is most interested in simulation outputs  
1012 for which observations are not available (e.g., unobserved or insufficiently observed properties  
1013 or fluxes in the past, properties and fluxes in the future); hence, standard procedures and  
1014 metrics for model validation (Section 3.2) are not helpful for this aspect. Uncertainty estimates  
1015 could be based on extensive model parameter and configuration sensitivity studies and  
1016 comparisons with models that include more realistic representations of uncertain or  
1017 parameterized processes. Furthermore, since specification of uncertainty is an integral part of

1018 DA, DA methodologies provide a useful framework for estimating uncertainty, especially  
1019 ensemble-based methods.

1020

1021 Any DA application requires uncertainty specification of the observations that are assimilated  
1022 and can provide uncertainty estimates of the results of the assimilation procedure. Specification  
1023 of uncertainty in the input data is necessary to inform the DA machinery about how much  
1024 weight and reach each data point or data type should have in influencing the outcome. The  
1025 more realistic the uncertainties of the input data, the better the DA outcomes in terms of  
1026 explanatory or predictive skill. It is important to note that “better” does not mean more precise  
1027 in this context. Overconfidence in the accuracy of assimilated observations will lead to  
1028 overfitting and a degradation of predictive skill. In the case of parameter optimization, the  
1029 output of the assimilation exercise is a set of optimized parameters. The uncertainty of optimal  
1030 parameters, referred to as *a posteriori* errors, is determined by a Hessian analysis of the cost  
1031 function in combination with the uncertainty of the input parameters before optimization, the  
1032 so-called *a priori* errors (Thacker et al. 1989, Fennel et al. 2001). In the case of ensemble-based  
1033 state estimation, the ensemble spread of the reanalyzed model state provides a spatially and  
1034 temporally resolved estimate of the uncertainty of the reanalysis (Yu et al. 2018, Hu et al. 2012).

1035

1036 However, an important caveat is that subjectivity enters the uncertainty specification in all of  
1037 these approaches. For example, in the case of parameter optimization the assumed *a priori*  
1038 errors, their probability distributions, and the choice of the cost function are subjective and  
1039 influence the *a posteriori* errors (but interestingly the values of the observations themselves do  
1040 not). In the case of ensemble-based state estimation, the sources of uncertainty inherent in the  
1041 model simulation have to be specified and simulated by generating variations within a model  
1042 ensemble. Sources of uncertainty include errors in atmospheric forcing and boundary  
1043 conditions, model parameters, and structural uncertainty. Uncertainty in forcing and boundary  
1044 conditions is often represented by perturbing the time of sampling, uncertainty in parameters is  
1045 represented by sampling from a probability distribution (based on *a priori* assumptions about  
1046 the uncertainty of each parameter), and the structural uncertainty is typically represented via  
1047 brute-force inflation factors that amplify ensemble spread. Yu et al. (2019), Li et al. (2016), and  
1048 Thacker et al. (2012) provide examples where different sources of model uncertainty are  
1049 accounted for. While the mechanics by which the model ensemble is generated and spreads  
1050 over time is thus subjective, grossly inappropriate choices will lead to obviously wrong or  
1051 degraded reanalyses. The success of a DA exercise, which is best judged by an evaluation of  
1052 whether the predictive power of the model has improved, thus provides a useful reality check  
1053 on whether the choices for specifying uncertainty were appropriate.

1054

1055 How can the framework for specifying and estimating uncertainty from model ensembles be  
1056 applied in the context of OAE research? Two different cases should be considered here: 1)  
1057 model applications where the absolute value of quantities matters for the research question to  
1058 be addressed and thus the uncertainty of the simulated output, and 2) applications where  
1059 information about the difference between a simulation with and without OAE is of interest and  
1060 the uncertainty of this difference (e.g., the net CO<sub>2</sub> uptake and its uncertainty in the context of

1061 MRV). Examples of the first case include studies of the stability of added alkalinity (i.e.,  
1062 simulation of runaway calcium carbonate precipitation) and studies about the exposure of  
1063 planktonic and benthic communities to high pH. In this case, the ensemble framework  
1064 described above can be applied with the caveat that the specification of all the relevant sources  
1065 of uncertainty is by no means trivial and subjective to some degree.

1066  
1067 The second case is highly relevant for MRV of OAE where one is interested in accurately  
1068 quantifying the increase in seawater DIC due to OAE with well characterized uncertainty. In  
1069 this case, one would use two simulations that are based on an identical model set-up with only  
1070 one difference, namely a source of alkalinity is applied to one (i.e., one of these two simulations  
1071 is counterfactual or hypothetical, the other would typically be as realistic as possible). It may be  
1072 tempting, and is conceptually straightforward, to apply the ensemble framework for each  
1073 model of the pair and combine the resulting uncertainties via error propagation. However, in  
1074 practice this would not provide meaningful estimates because there are sources of uncertainty  
1075 that are unaffected by OAE (e.g., atmospheric forcing) and accounting for them may  
1076 significantly overestimate uncertainty in the estimated net CO<sub>2</sub> uptake. A more appropriate  
1077 approach would be to construct an ensemble of model pairs that explicitly accounts for  
1078 uncertainty related to the impacts of alkalinity addition. How to specify and simulate the  
1079 sources of uncertainty directly resulting from OAE in practice remains an open research  
1080 question.

## 1081 1082 **4 Model experimentation**

1083 In this section, we lay out general objectives for model experimentation in the context of OAE  
1084 research and provide a short historical view of how these model studies have evolved (Section  
1085 4.1) followed by specific recommendations for Observing System Simulation Experiments  
1086 (Section 4.2) and model intercomparisons (Section 4.3).

### 1087 1088 **4.1 General objectives of model experimentation**

1089 General objectives of OAE modeling include (1) gaining a better understanding of the  
1090 biogeochemistry of OAE, including its effectiveness and side effects, (2) supporting  
1091 experiments, field trials, or commercial deployments including through the optimization of  
1092 observing systems, (3) assessing global carbon-cycle and climate feedbacks, (4) understanding  
1093 the role that OAE can play in climate mitigation efforts, and (5) supporting monitoring,  
1094 reporting, and verification activities. At a conceptual level, model approaches for OAE can be  
1095 classified as belonging into one of two groups: idealized or realistic. Idealized modeling  
1096 approaches are typically driven by research questions of a fundamental nature and aim to  
1097 develop or test hypotheses or provide improved process understanding while strongly  
1098 simplifying a range of potentially complicating factors. They are useful for illustrating cause-  
1099 and-effect relationships and the range of plausible outcomes given strong assumptions. In  
1100 contrast, realistic modeling approaches aim to include a broad range of contributing factors as  
1101 accurately as possible and provide detailed hindcasts or predictions that, if the model has skill,  
1102 can be used for a range of practical applications. In practice, the dividing line between idealized

1103 and realistic models is blurry. Of course, no model will ever simulate all aspects of reality,  
1104 hence even realistic simulations make many assumptions and are prone to errors from multiple  
1105 sources. It can be effective to apply idealized and realistic approaches in a complementary  
1106 manner and iteratively.

1107 It is illustrative to review briefly how modeling for OAE research has developed over the course  
1108 of the last decade. Much of the early work on OAE used idealized models. Model simulations  
1109 were designed to investigate whether the theoretical concept of OAE could remove large  
1110 amounts of CO<sub>2</sub> on the global scale. Rather than trying to account for the technical and socio-  
1111 economic constraints of OAE deployment, the model experiments were designed to investigate  
1112 what would happen if surface alkalinity was homogeneously increased by massive amounts via  
1113 a constant addition rate over extremely large regions of the ocean, e.g., in all sea-ice free waters  
1114 (Paquay and Zeebe, 2013; Keller et al., 2014; Ilyina et al., 2013; Köhler et al., 2010; Köhler et al.,  
1115 2013). These simulated OAE deployments will never be realized, but the model results  
1116 suggested that OAE can be viable as a CDR approach. A particular advantage of this idealized  
1117 approach is that the effect of OAE was easy to detect against internal model variability, i.e., the  
1118 signal to noise ratio is high. The next steps in modeling OAE have remained idealized but have  
1119 begun to introduce more constraints and better mechanistic or empirically derived components  
1120 as experimental OAE data becomes available. Recently, modeling studies tailored to specific  
1121 regions and modes of application have been conducted to support field trials or commercial  
1122 deployment (Mongin et al. 2021, Wang et al. 2023). These applications must be as realistic as  
1123 possible. None of the modeling studies published to date have simulated an actual OAE field  
1124 trial.

#### 1125 **4.2 Recommendations for Observing System Simulation Experiments (OSSEs)**

1126 Observing system simulation experiments (OSSEs) use data-assimilative simulations to design  
1127 new, or modify existing, observing systems such that deployments of observing assets, e.g.,  
1128 floats, gliders, moorings, or surface vehicles, is optimized. General overviews and best practices  
1129 for OSSEs are provided by Halliwell et al. (2015) and Hoffman and Atlas (2016). Examples of  
1130 applications to biogeochemical models include Ford (2021), Wang et al. (2020), and Denvil-  
1131 Sommer et al. (2021). Their goal is to maximize the information gained from a new or modified  
1132 observing system, while keeping the number of required instruments, sensors, or deployments  
1133 – and thereby cost and effort – low. OSSEs are especially valuable tools in the context of OAE  
1134 research because the marine carbonate system is still undersampled, observing systems need to  
1135 be designed and expanded, and new instruments deployed and configured (Boyd et al. 2023).

1136 In practice, this is done with the help of a pair of two different models or model versions, also  
1137 referred to as twin experiments, as follows. A simulation of one of the models is considered to  
1138 be the “truth.” This simulation is also referred to as the “nature run” and synthetic observations  
1139 are generated by subsampling this nature run. This subsampling can be repeated with different  
1140 sampling schemes (e.g., different variable types, different numbers of profiles, transects, and/or  
1141 fixed location time series, etc.) to represent different configurations of the observing system.  
1142 Finally, the synthetic observations are assimilated into the other model for which a non-

1143 assimilative simulation, the so-called “free run,” is also available. The skill of this data-  
1144 assimilative simulation, also referred to as the “forecast run,” can be assessed against the free  
1145 run using independent observations that are also sampled from the nature run. In this way the  
1146 impact of different sets of observations on the data-assimilative model can be measured and  
1147 assessed.

1148 While conceptually straightforward, care and consideration are required when setting up  
1149 OSSEs. For example, the choice of the two model versions making up the twin is important. If  
1150 the models chosen for the truth and forecast runs are versions of the same model  
1151 implementation that were generated by perturbing initial, forcing or boundary conditions in  
1152 one of them, the method is referred to as the “identical twin” approach. If two different model  
1153 types are used, they are “non-identical twins.” The intermediate approach where the same  
1154 model type is used but in different configurations (e.g., different physical parameterizations  
1155 and/or spatial resolution) is referred to as fraternal twin. The identical twin approach has been  
1156 more common in oceanic DA applications although atmospheric OSSEs have shown that it can  
1157 provide biased impact assessments (Hoffman and Atlas, 2016) typically because the error  
1158 growth rate between the truth and forecast runs is insufficient. A direct comparison of the non-  
1159 identical and identical twin approach for an ocean circulation model of the Gulf of Mexico has  
1160 been conducted by Yu et al. (2019). In their assessment of the impacts of the existing observing  
1161 system (consisting of satellites and Argo floats), the identical twin approach provided overly  
1162 optimistic improvements in model skill after assimilation of data from some observing assets  
1163 (specifically sea-surface height and temperature) but undervalued the contribution from  
1164 temperature and salinity profiles. They concluded that skill assessments and OSSEs using the  
1165 non-identical twin approach are more robust. Similar concerns likely apply to OSSEs for  
1166 biogeochemical properties, but this remains to be studied systematically.

### 1167 **4.3 Recommendations for intercomparisons**

1168 A common approach to assessing model uncertainty are coordinated, multi-model studies,  
1169 commonly called model intercomparison projects or MIPs. They can be used to explore the  
1170 simulated range of model behaviors, to isolate the strengths and weaknesses of different models  
1171 in a controlled setting, and to interpret, through idealized experiments, inter-model differences  
1172 (IPCC 2013). Carefully designed experiments can also offer a way to distinguish between errors  
1173 particular to an individual model and those that might be more universal and should become  
1174 priority targets for model improvement (IPCC 2013). These studies rely on common agreed-  
1175 upon protocols for simulating certain processes and writing of diagnostic output to ensure that  
1176 best practices are followed, and results are comparable (e.g., Griffies et al., 2016). The best-  
1177 known model intercomparison project is probably the Coupled Model Intercomparison Project  
1178 (CMIP, Eyring et al., 2016), which is currently finishing up its 6<sup>th</sup> phase. Within CMIP6, the  
1179 carbon dioxide removal intercomparison project (CDRMIP; Keller et al., 2018) is the first project  
1180 to develop a model intercomparison experiment for ocean alkalinity enhancement. This and  
1181 other MIP examples, including those conducted at smaller region scales (Wilcox et al., 2022),  
1182 provide a blueprint for developing coordinated multi-model experiments.

1183 The following key practices have proven useful in previous coordinated multi-model  
1184 comparisons. Since broad participation is typically desired, the protocol should be  
1185 straightforward for modeling groups to implement, otherwise few will have the resources to  
1186 participate. In practice this means avoiding new implementations of complex code or requiring  
1187 too many or too long simulations. If applicable, forcing data should be centrally prepared and  
1188 provided to participants in a standardized way that enables easy modification or reformatting,  
1189 if needed, for use with different models. Using common simulations that modeling groups are  
1190 likely to have completed already, e.g., climate change scenarios, as control runs and  
1191 experimental branching points is helpful for minimizing the number of additional required  
1192 simulations. It is useful to establish common practices that facilitate the production and analysis  
1193 of the model output, e.g., what should be archived and shared (Jukes et al., 2020) and data  
1194 standards governing the structure and required metadata for model output (Pascoe et al., 2020).  
1195 Shared software to standardize model output, such as the Climate Model Output Rewriter  
1196 (CMOR; <https://cmor.llnl.gov/>) commonly used in CMIP, can be helpful. To maximize the use of  
1197 model output, it should be made available for public download with digital object identifiers  
1198 (DOIs). The Earth System Grid Federation (ESGF) is an example of such a system (Petrie et al.,  
1199 2021). If applicable, preparing and providing quality-controlled observational datasets for  
1200 model evaluation is useful for facilitating analytical efforts (Waliser et al., 2020). Coordinating  
1201 the analysis is helpful to avoid duplicative efforts and ensure consistent application of  
1202 evaluation metrics. Finally, the design of a coordinated multi-model experiment and all its  
1203 procedures should be well documented in publications or permanently archived protocols. It is  
1204 advisable to test the multi-model experiment with a small subset of models, before inviting a  
1205 large number of participants. Furthermore, it is worth remembering that the science questions  
1206 must be appropriate. MIPs require much effort and not every science question needs a MIP to  
1207 be answered.

## 1208 **5 Summary and Key Recommendations**

1209 A range of modeling tools and analysis methods are available for OAE research to address  
1210 questions from micro- to global scales; however, each of these tools and methods has limitations  
1211 and caveats that model users and users of model-generated outputs need to be aware of.  
1212 Furthermore, this new field of research poses questions and challenges that current tools were  
1213 not designed to address, necessitating further development.

1214  
1215 A common objective of all modeling approaches described in this article is to simulate the  
1216 spatio-temporal evolution of carbon chemistry properties in seawater by accounting for the  
1217 physical, chemical, and biological processes that determine this evolution. Idealized models,  
1218 which neglect some aspects of reality in the interest of simplicity and clarity of assumptions,  
1219 have long been used to test basic questions about OAE. As research questions are becoming  
1220 more focussed on the practical aspects, feasibility, and ecosystem impacts of OAE, more realistic  
1221 models are increasingly desirable. A skillful realistic model can provide spatial and temporal  
1222 context for observations, including estimates of properties and fluxes not directly observed.  
1223 Such model will include parameterizations of the relevant processes for the research objective to  
1224 be addressed and will be constrained by observations that contain sufficient meaningful



1225 information. However, model formulations of several properties and processes relevant to OAE  
1226 research remain uncertain or highly simplified. For example, presently used model  
1227 representations of alkalinity in seawater are likely inadequate and may require explicit  
1228 representation of at least some of the multiple biotic and abiotic sources and sinks of alkalinity;  
1229 the mechanisms and triggers for spontaneous calcium carbonate precipitation are only  
1230 beginning to be described and not yet represented in models; and the impacts of pH  
1231 perturbations on plankton diversity and trophic interactions remain an active area of study and  
1232 unaccounted in biogeochemical models. Furthermore, it is difficult to obtain solid constraints on  
1233 the seawater carbonate system, especially in sufficient spatial and temporal resolution for  
1234 robust model validation and DA. Theoretically, knowledge of two of the carbonate system  
1235 parameters allows calculation of the others, but unfortunately  $p\text{CO}_2$  and pH, the pair most  
1236 accessible to autonomous measurement, results in high uncertainties.

1237 One inherent challenge to OAE research is the multiscale nature of many of the relevant  
1238 questions. Different modelling tools are available for different spatial scales. While some  
1239 research questions may fall neatly within the limited spatial range of a particular model, many  
1240 do not and require a bridging of scales that could be accomplished via new parameterizations  
1241 yet to be developed or dynamic coupling of different modeling tools. It is important to  
1242 emphasize that models have to be tailored to the questions they are meant to address. This  
1243 means considering what level of model complexity is required and seeking parsimonious  
1244 representations that are well-supported by empirical constraints.

1245  
1246 It is important to note that even after thorough validation, any model simulation will be prone  
1247 to errors and uncertainties due to inaccuracies in model inputs, structural uncertainty due to  
1248 numerical approximation schemes and insufficient process understanding or representation,  
1249 and inaccurate model parameters and parameterizations. Deviations between models and  
1250 reality can be reduced by DA, which is typically applied either to systematically optimize  
1251 model parameters or to produce optimal estimates of the ocean state. Optimization of model  
1252 parameters addresses systematic model errors and biases; it is useful for systematic testing of  
1253 different model formulations during model design. State estimation assumes an unbiased  
1254 model and addresses unresolved stochasticity, thus leading to model states that are in better  
1255 agreement with the observed ocean state. However, successful application of DA critically  
1256 requires sufficient observations. Currently, the biggest impediment to implementing data-  
1257 assimilative models for OAE research is the sparsity of carbonate system observations. OSSEs,  
1258 data-assimilative simulations that inform how to place observing assets most effectively, will  
1259 prove useful in this context. It should also be noted that assimilation of carbonate system  
1260 parameters is not appropriate when models are applied for MRV.

1261  
1262 Uncertainty analysis is a necessary component of any quantitative research and will be an  
1263 essential deliverable for effective approaches to MRV. Ensemble-based DA methodologies  
1264 provide a useful framework for estimating uncertainty. Consideration of this framework  
1265 illustrates the “law of conservation of difficulty” applies here. Quantitative assumptions about  
1266 the uncertainty distributions of input data and input parameters, and of structural uncertainties

1267 inherent in the model are required to obtain an uncertainty estimate of the model output, in  
1268 other words, difficult assumptions about errors have to be made somewhere. A common  
1269 approach to assessing model uncertainty is by coordinated, multi-model intercomparison. Such  
1270 studies can be used to explore the range of simulated behaviors and the strengths and  
1271 weaknesses of different models and, by elucidating inter-model differences, they can offer  
1272 guidance on priority targets for model improvement.

1273

1274 Key recommendations arising from this article are as follows:

1275

1276 • Idealized models of particle-fluid interaction are recommended to address questions  
1277 about dissolution and precipitation kinetics at the scale of particles, realistic local-scale  
1278 models are recommended for addressing questions about nearfield processes in the  
1279 turbulent environment around injection sites, and larger-scale regional or global ocean  
1280 models are recommended to support observational design for field experiments, to  
1281 demonstrate possible verification frameworks, and to address questions about global-  
1282 scale feedbacks on ocean biogeochemistry.

1283 • When simulating OAE approaches that may generate high oversaturation with respect  
1284 to carbonate, spontaneous precipitation of carbonates needs to be considered and  
1285 appropriate approaches should be developed, e.g., using near-field models to  
1286 mechanistically represent this process and a meta-model approach to develop  
1287 parameterizations that are suitable for far-field and larger-scale models.

1288 • Shortcomings in current-generation models in terms of representing physiological  
1289 responses of the plankton community to OAE (especially when using crushed-rock  
1290 feedstocks) need to be recognized, better qualified, and addressed. Empirical research  
1291 exploring physiological sensitivities should be used to develop prioritizations of key  
1292 model processes comprising early targets for implementation.

1293 • The exchange of solutes between the sediments and overlying water influences the  
1294 seawater carbonate system with DIC from the remineralization of organic matter being  
1295 returned to overlying water (and alkalinity if this remineralization occurs anaerobically),  
1296 dissolution of  $\text{CaCO}_3$  releasing alkalinity, and burial of  $\text{CaCO}_3$  acting as alkalinity sink.  
1297 Accounting for these exchanges between sediments and overlying water and its  
1298 variability on tidal, seasonal, interannual, and millennial timescales will likely be  
1299 necessary in regional and global biogeochemical models that aim to simulate alkalinity  
1300 cycling.

1301 • River inputs of alkalinity and DIC in regional and global ocean biogeochemical models,  
1302 including fluxes resulting from land-based CDR applications, should be accurately  
1303 accounted for. Efforts should be made to improve quantification of riverine fluxes  
1304 resulting from ongoing field trials and commercial applications, and to establish  
1305 initiatives to effectively track the solute additions from terrestrial alkalinity  
1306 enhancements.

- 1307 • When simulating large-scale deployment of OAE in ocean-only models with prescribed  
1308 atmospheric CO<sub>2</sub>, the subtle changes in the atmospheric CO<sub>2</sub> inventory resulting from  
1309 CDR should be accounted for.
- 1310 • Models should be tailored to the specific questions they are meant to address while  
1311 seeking parsimonious representations that are well-supported by empirical constraints.  
1312 For example, for the purpose of MRV it may be appropriate to neglect biological  
1313 dynamics since the core target is to capture the net air-sea CO<sub>2</sub> exchange associated with  
1314 the OAE-induced surface ocean *p*CO<sub>2</sub> anomaly.
- 1315 • Model validation should be an integral part of model implementation and application.  
1316 For OAE research, validation is a two-step challenge. First, it is necessary to validate  
1317 unperturbed model baselines to gain confidence that the natural variability is  
1318 represented appropriately and to quantify model uncertainties. Second, it should be  
1319 verified that the model accurately represents the perturbations of an alkalinity addition.
- 1320 • Since no single model validation metric provides a complete picture of a model's skill,  
1321 multiple complementary metrics should be used in combination. Furthermore, different  
1322 points in space and time, and a breadth of variable types should be part of any  
1323 comprehensive validation.
- 1324 • Data assimilation, the process of improving the dynamical behavior of models by  
1325 statistically combining them with observations, should be employed in order to obtain  
1326 the most accurate model simulations possible, e.g., to optimize model parameters or to  
1327 estimate the ocean state. The former addresses systematic errors and biases in models,  
1328 while the latter assumes an unbiased model and addresses unresolved stochasticity.
- 1329 • When applying data-assimilative models for quantification of the OAE-induced net CO<sub>2</sub>  
1330 uptake by calculating the difference between a realistic and a counterfactual simulation,  
1331 it is not appropriate to assimilate biogeochemical observations of properties affected by  
1332 the alkalinity enhancement as this would eliminate the ability to make valid  
1333 comparisons between the two simulations. However, assimilation of observations that  
1334 are unaffected by OAE can be applied to both simulations of the pair.
- 1335 • Successful application of DA critically requires sufficient observations either of the  
1336 properties that the model parameters to be estimated depend on or of the state variables  
1337 that are being estimated. Observing System Simulation Experiments are recommended  
1338 to design observing strategies tailored to the needs of specific OAE applications.
- 1339 • Model results should be paired with sound qualitative and quantitative uncertainty  
1340 estimates, especially when used for practical decisions. DA methodologies provide a  
1341 useful framework for estimating uncertainty, especially ensemble-based methods.  
1342 Another common approach to assessing model uncertainty are coordinated, multi-  
1343 model studies, commonly called model intercomparison projects or MIPs.

1344

1345 **Acknowledgements**

1346 We thank the Ocean Acidification and other ocean Changes – Impacts and Solutions (OACIS),  
1347 an initiative of the Prince Albert II of Monaco Foundation, Judith Meyer, and Angela Stevenson  
1348 for their support throughout the project. We extend our gratitude to the Villefranche  
1349 Oceanographic Laboratory for supporting the meeting of the lead authors in January 2023.  
1350 Jessica Oberlander’s assistance in compiling the bibliography is gratefully acknowledged.

1351

1352 **Competing interests**

1353 KF, AL, and CA are collaborating with Planetary Technology, a climate-tech company, and Pro-  
1354 Oceanus Systems Inc., an ocean technology company, as part of an NSERC Alliance Missions  
1355 project focussed on OAE; none of the partners have made direct financial contributions to the  
1356 project. RM and JO are collaborating with Planetary Technologies, and JO is partially supported  
1357 by Planetary Technologies via an NSERC Alliance grant. ML is the Executive Director of  
1358 [C]Worthy, LLC, which is a non-profit research organization focused on building tools to  
1359 support MRV for ocean CDR. Competing interests are declared in a summary for the entire  
1360 volume at: [\url{https://sp.copernicus.org/articles/sp-bpoae-ci-summary.zip}](https://sp.copernicus.org/articles/sp-bpoae-ci-summary.zip).

1361

1362 **Financial support**

1363 The compilation of this article has been supported by the ClimateWorks Foundation (grant no.  
1364 22-0296) and the Prince Albert II of Monaco Foundation. KF, AL, RM, and JO acknowledge  
1365 funding by NSERC’s Discovery and Alliance Programs. KF, DK, AL, and AO are supported by  
1366 the Ocean Alk-Align project funded by Carbon to Sea. RM is supported by the Canada Research  
1367 Chairs Program. JPM is supported by the Simons Collaboration on Computational  
1368 Biogeochemical Modeling of Marine Ecosystems (grant ID: 459949FY22) and the NOAA Ocean  
1369 Acidification Program (grant ID: NA19OAR0170357). DBW is supported by the NASA Earth  
1370 science New Investigator Program.

1371 **References**

1372

1373 Aller, R. C.: Transport and reactions in the bioirrigated zone, in: *The Benthic Boundary Layer*,  
1374 edited by: Boudreau, B. P., and Jorgensen, B. B., Oxford University Press, 269-301, ISBN  
1375 9780195118810, 2001.

1376 Bach, L. T., Gill, S. J., Rickaby, R. E., Gore, S., and Renforth, P.: CO<sub>2</sub> Removal With Enhanced  
1377 Weathering and Ocean Alkalinity Enhancement: Potential Risks and Co-benefits for Marine  
1378 Pelagic Ecosystems, *Front. Clim.*, 1, <https://doi.org/10.3389/fclim.2019.00007>, 2019.

1379 Barrett, P. M., Resing, J. A., Buck, N. J., Freely, R. A., Bullister, J. L., Buck, C. S., and Landing, W.  
1380 M.: Calcium carbonate dissolution in the upper 1000 m of the eastern North Atlantic, *Global*  
1381 *Biogeochem. Cy.*, 28, 386-397, <https://doi.org/10.1002/2013GB004619>, 2014.

1382 Barton, A. D., Pershing, A. J., Litchman, E., Record, N. R., Edwards, K. F., Kinkel, Z. V., Kiørboe,  
1383 T., and Ward, B. A.: The biogeography of marine plankton traits, *Ecol. Lett.*, 16, 522-534,  
1384 <https://doi.org/10.1111/ele.12063>, 2013.

1385 Bates, N. R., and Merlivat, L.: The influence of short-term wind variability on air-sea CO<sub>2</sub>  
1386 exchange, *Geophys. Res. Lett.*, 28, 3281-3284, <https://doi.org/10.1029/2001GL012897>, 2001.

1387 Bell, T. G., Landwehr, S., Miller, S. D., de Bruyn, W. J., Callaghan, A. H., Scanlon, B., Ward, B.,  
1388 Yang, M., and Saltzman, E. S.: Estimation of bubble-mediated air-sea gas exchange from  
1389 concurrent DMS and CO<sub>2</sub> transfer velocities at intermediate-high wind speeds, *Atmos. Chem.*  
1390 *Phys.*, 17, 9019-9033, <https://doi.org/10.5194/acp-17-9019-2017>, 2017.

1391 Bittig, H. C., Steinhoff, T., Claustre, H., Fiedler, B., Williams, N. L., Sauzède, R., Körtzinger, A.,  
1392 and Gattuso, J.-P.: An Alternative to Static Climatologies: Robust Estimation of Open Ocean  
1393 CO<sub>2</sub> Variables and Nutrient Concentrations From T, A, and O<sub>2</sub> Data Usin Baysian Neural  
1394 Networks, *Front. Mar. Sci.*, 5, 328, <https://doi.org/10/3389/fmars.2018.00328>, 2018.

1395 Bleninger, T., and Jirka, G. H.: Near- and far-field model coupling methodology for wastewater  
1396 discharges, *Proceedings of the 4th International Symposium in Environmental Hydraulics &*  
1397 *14th Congress of Asia and Pacific Division, International Association of Hydraulic Engineering*  
1398 *and Research*, 15-18, <https://doi.org/10.1201/b16814-73>, 2004.

1399 Boudreau, B. P. (Eds.): *Diagenetic Models and their Implementation: Modelling Transport and*  
1400 *Reactions in Aquatic Sciences*, Springer, <https://do.org/10.I007/978-3-642-60421-8>, 1997.

1401 Boudreau, B. P., Middelburg, J. J., and Meysman, F. J. R.: Carbonate compensation dynamics,  
1402 *Geophys., Res. Lett.*, 37, <https://doi.org/10.1029/2009GL041847>, 2010.

1403 Boudreau, B. P., Middelburg, J. J., and Luo, Y.: The role of calcification in carbonate  
1404 compensation, *Nat. Geosci.*, 11, 894-900, <https://doi.org/10.1038/s41561-018-0259-5>, 2018.

1405 Boyd, P.W., Claustre, H., Legendre, L., Gattuso, J.-P., and Le Traon, P.-Y.: Operational  
1406 monitoring of open-ocean carbon dioxide removal deployments: Detection, attribution, and  
1407 determination of side effects, in: *Frontiers in Ocean Observing: Emerging Technologies for*  
1408 *Understanding and Managing a Changing Ocean*, edited by: Kappel, E. S., Cullen, V., Costello,  
1409 M. J., Galgani, L., Gordó-Vilaseca, C., Govindarajan, A., Kouhi, S.,  
1410 Lavin, C., McCartin, L., Müller, J. D., Pirenne, B., Tanhua, T., Zhao, Q., and Zhao, S.,  
1411 *Oceanography*, 36(Supplement 1), 2–10, <https://doi.org/10.5670/oceanog.2023.s1.2>, 2023.

1412 Briggs, E. M., Sandoval, S., Erten, A., Takeshita, Y., Kummel, A. C., and Martz, T. R.: Solid state  
1413 sensor for simultaneous measurement of total alkalinity and pH of seawater, *ACS Sens.*, 2, 1302-  
1414 1309, <https://doi.org/10.1021/acssensors.7b00305>, 2017.

1415 Burdige, D. J.: Preservation of Organic Matter in Marine Sediments: Controls, Mechanisms, and  
1416 an Imbalance in Sediment Organic Carbon Budgets?, *Chem. Rev.*, 107, 467-485,  
1417 <https://doi.org/10.1021/cr050347q>, 2007.

1418 Burt, D. J., Fröb, F., and Ilyina, T.: The sensitivity of the marine carbonate system to regional  
1419 ocean Alkalinity Enhancement. *Front. Clim.*, 3, <https://doi.org/10.3389/fclim.2021.624075>, 2021.

1420 Bushinsky, S.M., Takeshita, Y., and Williams, N. L.: Observing changes in ocean carbonate  
1421 chemistry: Our autonomous future, *Current Climate Change Reports* 5, 207–220,  
1422 <https://doi.org/10.1007/s40641-019-00129-8>, 2019.

1423 Carrassi, A., Bocquet, M., Bertino, L., and Evensen, G.: Data assimilation in the geosciences: An  
1424 overview of methods, issues, and perspectives, *WIREs Clim Change*, 9,  
1425 <https://doi.org/10.1002/wcc.535>, 2018.

1426 Carroll, D., Menemenlis, D., Adkins, J. F., Bowman, K. W., Brix, H., Dutkiewicz, S., Fenty, I.,  
1427 Gierach, M. M., Hill, C., Jahn, O., Landschützer, P., Lauderdale, J. M., Liu, J., Manizza, M.,  
1428 Naviaux, J. D., Rödenbeck, C., Schimel, D. S. Van der Stockem T., and Zhang, H.: The ECCO-  
1429 Darwin data-assimilative global ocean biogeochemistry model: Estimates of seasonal to  
1430 multidecadal surface ocean  $p\text{CO}_2$  and air-sea  $\text{CO}_2$  flux, *J. Adv. Model. Earth Sy.*, 12,  
1431 e2019MS001888. <https://doi.org/10.1029/2019MS001888>, 2020.

1432 Caserini, S., Pagano, D., Campo, F., Abbà, A., De Marco, S., Righi, D., Renforth, P., and Grosso,  
1433 M.: Potential of maritime transport for ocean liming and atmospheric  $\text{CO}_2$  removal, *Front.*  
1434 *Clim.*, 3, <https://doi.org/10.3389/fclim.2021.575900>, 2021.

1435 Ciavatta, S., Brewin, R. J. W., Skákala, J., Polimene, L., de Mora, L., Artioli, Y., and Allen, J. I.:  
1436 Assimilation of ocean-color plankton functional types to improve marine ecosystem  
1437 simulations, *J. Geophys. Res. Oceans*, 123, 834–854, <https://doi.org/10.1002/2017JC013490>, 2018.

1438 Chai, F., Johnson, K. S., Claustre, H., Xing, X., Wang, Y., Boss, E., Riser, S., Fennel, K., Schofield,  
1439 O., and Sutton, A.: Monitoring ocean biogeochemistry with autonomous platforms, *Nat. Rev.*  
1440 *Earth Environ.*, 1, 315–326, <https://doi.org/10.1038/s43017-020-0053-y>, 2020.

1441 Chang, Y. S., and Scotti, A.: Modeling unsteady turbulent flows over ripples: Reynolds-  
1442 averaged Navier-Stokes equations (RANS) versus large-eddy simulation (LES), *J. Geophys.*  
1443 *Res.-Oceans*, 109, C9, <https://doi.org/10.1029/2003JC002208>, 2004.

1444 Chua, E. J., Huettel, M., Fennel, K., and Fulweiler, R. W.: A case for addressing the unresolved  
1445 role of permeable shelf sediments in ocean denitrification, *Limnol. Oceanogr. Letters*, 7, 11-25  
1446 <https://doi.org/10.1002/lol2.10218>, 2022.

1447 CMEMS 2023. Global Ocean Physics Analysis and Forecast. E.U. Copernicus Marine Service  
1448 Information (CMEMS). Marine Data Store (MDS). DOI: 10.48670/moi-00016 (Accessed on 06-10-  
1449 2023)

1450 Cossarini, G., Mariotti, L., Feudale, L., Mignot, A., Salon, S., Taillandier, V., Teruzzi, A., and  
1451 D'Ortenzio, F.: Towards operational 3D-Var assimilation of chlorophyll Biogeochemical-Argo  
1452 float data into a biogeochemical model of the Mediterranean Sea, *Ocean Modell*, 133, 112–128,  
1453 <https://doi.org/10.1016/j.ocemod.2018.11.005>, 2019.

1454 Cullison Gray, S. E., DeGrandpre, M. D., Moore, T. S., Martz, T. R., Friederich, G. E., and  
1455 Johnson, K. S.: Applications of *in situ* pH measurements for inorganic carbon calculations, *Mar.*  
1456 *Chem.*, 125, 82-90, <https://doi.org/10.1016/j.marchem.2011.02.005>, 2011.

1457 Denvil-Sommer, A., Gehlen, M., and Vrac, M.: Observation system simulation experiments in  
1458 the Atlantic Ocean for enhanced surface ocean pCO<sub>2</sub> reconstructions, *Ocean Sci.*, 17, 1011–1030,  
1459 <https://doi.org/10.5194/os-17-1011-2021>, 2021.

1460 Dickson, A. G., and Riley, J. P.: The estimation of acid dissociation constants in seawater media  
1461 from potentiometric titrations with strong base. I. The ionic product of water -  $K_w$ , *Mar. Chem.*,  
1462 7, 89-99, [https://doi.org/10.1016/0304-4203\(79\)90001-X](https://doi.org/10.1016/0304-4203(79)90001-X), 1979.

1463 Doney, S. C., Lima, I., Moore, J. K., Lindsay, K., Behrenfeld, M. J., Westberry, T. K., Mahowald,  
1464 N., Glover, D. M., and Takahashi, T.: Skill metrics for confronting global upper ocean  
1465 ecosystem-biogeochemistry models against field and remote sensing data, *J. Mar. Syst.*, 76, 95-  
1466 112, <https://doi.org/10.1016/j.jmarsys.2008.05.015>, 2009.

1467 Dowd, M., Jones, E., and Parslow, J.: A statistical overview and perspectives on data  
1468 assimilation for marine biogeochemical models, *Environmetrics*, 25, 203-213,  
1469 <https://doi.org/10.1002/env.2264>, 2014.

1470 ECMWF 2023. European Centre for Medium-Range Weather Forecasts (ECMWF) IFS CY41r2  
1471 high-resolution operational forecasts (Accessed on 06-10-2023).

1472 Emerson, S. R., and Archer, D.: Calcium carbonate preservation in the ocean, *Philos. T. R. Soc. S-*  
1473 *A.*, 331, 29-40, <https://doi.org/10.1098/rsta.1990.0054>, 1990.

1474 Eyring, V., Bony, S., Meehl, G. A., Senior, C. A., Stevens, B., Stouffer, R. J., and Taylor, K. E.:  
1475 Overview of the Coupled Model Intercomparison Project Phase 6 (CMIP6) experimental design

1476 and organization, *Geosci. Model Dev.*, 9, 1937–1958, <https://doi.org/10.5194/gmd-9-1937-2016>,  
1477 2016.

1478 Fairall, C. W., Hare, J. E., Edson, J. B., and McGillis, W.: Parameterization and  
1479 micrometeorological measurement of air-sea gas transfer, *Bound.-Lay. Meteorol.*, 96, 63-106,  
1480 <https://doi.org/10.1023/A:1002662826020>, 2000.

1481 Fakhraee, M., Li, Z., Planavsky, N. J., and Reinhard, C. T.: A biogeochemical model of mineral-  
1482 based ocean alkalinity enhancement: impacts on the biological pump and ocean carbon uptake,  
1483 *Environ. Res. Lett.*, 18, 044047, <https://doi.org/10.1088/1748-9326/acc9d4>, 2023.

1484 Farsoiyya, P. K., Magdelaine, Q., Antkowiak, A., Popinet, S., and Deike, L.: Direct numerical  
1485 simulations of bubble-mediated gas transfer and dissolution in quiescent and turbulent flows, *J.*  
1486 *Fluid Mech.*, 954, A29, <https://doi.org/10.1017/jfm.2022.994>, 2023.

1487 Fassbender, A. J. Sabine, C. L., Lawrence-Slavas, N., De Carlo, E. H., Meinig, C., and Maenner  
1488 Jones, S.: Robust sensor for extended autonomous measurements of surface ocean dissolved  
1489 inorganic carbon, *Environ. Sci. Technol.*, 49, 3628-3635, <https://doi.org/10.1021/es5047183>, 2015.

1490 Feng, E. Y., Koeve, W., Keller, D. P., and Oeschler, A.: Model-Based Assessment of the CO<sub>2</sub>  
1491 Sequestration Potential of Coastal Ocean Alkalinization, *Earth's Future*, 5, 1252-1266,  
1492 <https://doi.org/10.1002/2017EF000659>, 2017.

1493 Fennel, K., Losch, M., Schröter, J., and Wenzel, M.: Testing a marine ecosystem model:  
1494 sensitivity analysis and parameter optimization, *J. Marine Syst.*, 28, 45-63,  
1495 [https://doi.org/10.1016/S0924-7963\(00\)00083-X](https://doi.org/10.1016/S0924-7963(00)00083-X), 2001.

1496 Fennel, K., Wilkin, J., Previdi, M., and Najjar, R.: Denitrification effects on air-sea CO<sub>2</sub> flux in the  
1497 coastal ocean: Simulations for the Northwest North Atlantic, *Geophys. Res. Lett.*, 35, L24608,  
1498 <https://doi.org/10.1029/2008GL036147>, 2008.

1499 Fennel, K., Gehlen, M., Brasseur, P., Brown, C. W., Ciavatta, S., Cossarini, G., Crise, A.,  
1500 Edwards, C. A., Ford, D., Friedrichs, M. A. M., Gregoire, M., Jones, E., Kim, H-C., Lamouroux,  
1501 J., Murtugudde, R., Perruche, C., and the GODAE OceanView Marine Ecosystem Analysis and  
1502 Prediction Task Team: Advancing Marine Biogeochemical and Ecosystem Reanalyses and  
1503 Forecasts as Tools for Monitoring and Managing Ecosystem Health, *Front. Mar. Sci.*, 6, 89,  
1504 <https://doi.org/10.3389/fmars.2019.00089>, 2019.

1505 Fennel, K., Mattern, J. P., Doney, S., Bopp, L., Moore, A., Wang, B., and Yu, L.: Ocean  
1506 biogeochemical modelling, *Nat. Rev. Methods Primers*, 2, 76, <https://doi.org/10.1038/s43586-022-00154-2>, 2022.

1508 Ferderer, A., Chase, Z., Kennedy, F., Schulz, K. G., and Bach, L. T.: Assessing the influence of  
1509 ocean alkalinity enhancement on a coastal phytoplankton community, *Biogeosciences*, 19, 5375–  
1510 5399, <https://doi.org/10.5194/bg-19-5375-2022>, 2022.



1511 Foteinis, S., Campbell, J. S., and Renforth, P.: Life cycle assessment of coastal enhanced  
1512 weathering for carbon dioxide removal from air, *Environ. Sci. Technol.*, 57, 6169-6178,  
1513 <https://doi.org/10.1021/acs.est.2c08633>, 2023.

1514 Ford, D.: Assimilating synthetic Biogeochemical-Argo and ocean colour observations into a  
1515 global ocean model to inform observing system design, *Biogeosciences*, 18, 509–534,  
1516 <https://doi.org/10.5194/bg-18-509-2021>, 2021.

1517 Fornari, W., Picano, F., Sardinia, G., and Brandt, L.: Reduced particle settling speed in  
1518 turbulence, *J. Fluid Mech.*, 808, 153-167, <https://doi.org/10.1017/jfm.2016.648>, 2016.

1519 Fry, C. H., Tyrrell, T., Hain, M. P., Bates, N. R., and Achterberg, E. P.: Analysis of global surface  
1520 ocean alkalinity to determine controlling processes, *Mar. Chem.*, 174, 46-57,  
1521 <https://doi.org/10.1016/j.marchem.2015.05.003>, 2015.

1522 Fuhr, M., Geilert, S., Schmidt, M., Liebetrau, V., Vogt, C., Ledwig, B., and Wallmann, K.:  
1523 Kinetics of olivine weathering in seawater: an experimental study, *Front. Clim.*, 4,  
1524 <https://doi.org/10.3389/fclim.2022.831587>, 2022.

1525 Gehlen, M., Bopp, L., and Aumont, O.: Short-term dissolution response of pelagic carbonate  
1526 sediments to the invasion of anthropogenic CO<sub>2</sub>: A model study, *Geochem. Geophys. Geosy.*, 9,  
1527 <https://doi.org/10.1029/2007GC001756>, 2008.

1528 Gent, P. R., and McWilliams, J. C.: Isopycnal Mixing in Ocean Circulation Models, *J. Phys.*  
1529 *Oceanogr.*, 20, 150–155, [https://doi.org/10.1175/1520-0485\(1990\)020<0150:IMIOCM>2.0.CO;2](https://doi.org/10.1175/1520-0485(1990)020<0150:IMIOCM>2.0.CO;2),  
1530 1990.

1531 Gentile, E., Tarantola, F., Lockley, A., Vivian, C., and Caserini, S.: Use of aircraft in ocean  
1532 alkalinity enhancement, *Sci. Total Environ.*, 822, 153484,  
1533 <https://doi.org/10.1016/j.scitotenv.2022.153484>, 2022.

1534 Golshan, R., Tejada-Martínez, A. E., Juha, M. J., and Bazilevs, Y.: LES and RANS simulation of  
1535 wind-and wave-forced oceanic turbulent boundary layers in shallow water with wall modeling,  
1536 *Comput. Fluids*, 145, 96-108, <https://doi.org/10.1016/j.compfluid.2016.05.016>, 2017.

1537 Griffies, S. M., Danabasoglu, G., Durack, P. J., Adcroft, A. J., Balaji, V., Böning, C. W.,  
1538 Chassignet, E. P., Curchitser, E., Deshayes, J., Drange, H., Fox-Kemper, B., Gleckler, P. J.,  
1539 Gregory, J. M., Haak, H., Hallberg, R. W., Heimbach, P., Hewitt, H. T., Holland, D. M., Ilyina, T.,  
1540 Jungclaus, J. H., Komuro, Y., Krasting, J. P., Large, W. G., Marsland, S. J., Masina, S., McDougall,  
1541 T. J., Nurser, A. J. G., Orr, J. C., Pirani, A., Qiao, F., Stouffer, R. J., Taylor, K. E., Treguier, A. M.,  
1542 Tsujino, H., Uotila, P., Valdivieso, M., Wang, Q., Winton, M., and Yeager, S. G.: OMIP  
1543 contribution to CMIP6: experimental and diagnostic protocol for the physical component of the  
1544 Ocean Model Intercomparison Project, *Geosci. Model Dev.*, 9, 3231–3296,  
1545 <https://doi.org/10.5194/gmd-9-3231-2016>, 2016.

1546 Grigoratou, M., Monteiro, F. M., Wilson, J. D., Ridgwell, A., and Schmidt, D. N.: Exploring the  
1547 impact of climate change on the global distribution of non-spinose planktonic foraminifera  
1548 using a trait-based ecosystem model, *Glob. Change Biol.*, 28, 1063-1076,  
1549 <https://doi.org/10.1111/gcb.15964>, 2022.

1550 Guo, J. A., Strzepak, R., Willis, A., Ferderer, A., and Bach, L. T.: Investigating the effect of nickel  
1551 concentration on phytoplankton growth to assess potential side-effects of ocean alkalinity  
1552 enhancement, *Biogeosciences*, 19, 3683–3697, <https://doi.org/10.5194/bg-19-3683-2022>, 2022.

1553 Haidvogel, D. B., Arango, H., Budgell, W. P., Cornuelle, B. D., Curchitser, E., Lorenzo, E. D.,  
1554 Fennel, K., Geyer, W. R., Hermann, A. J., Lanerolle, L., Levin, J., McWilliams, J. C., Miller, A. J.,  
1555 Moore, A. M., Powell, T. M., Shchepetkin, A. F., Sherwood, C. R., Signell, R. P., Warner, J. C.,  
1556 and Wilkin, J.: Ocean forecasting in terrain-following coordinates: Formulation and skill  
1557 assessment of the Regional Ocean Modeling System, *J. Comput. Phys.*, 227, 3595-3624,  
1558 <https://doi.org/10.1016/j.jcp.2007.06.016>, 2008.

1559 Hain, M. P., Sigman, D. M., Higgins, J. A., and Haug, G. H.: The effects of secular calcium and  
1560 magnesium concentration changes on the thermodynamics of seawater acid/base chemistry:  
1561 Implications for Eocene and Cretaceous ocean carbon chemistry and buffering, *Global*  
1562 *Biogeochem. Cy.*, 29, 517-533, <https://doi.org/10.1002/2014GB004986>, 2015.

1563 Halliwell, G. R., Kourafalou, V., Le Hénaff, M., Shay, L. K., and Atlas, R.: OSSE impact analysis  
1564 of airborne ocean surveys for improving upper-ocean dynamical and thermodynamical  
1565 forecasts in the Gulf of Mexico, *Prog. Oceanogr.*, 130, 32–46,  
1566 <https://doi.org/10.1016/j.pocean.2014.09.004>, 2015.

1567 Hartmann, J., Suitner, N., Lim, C., Schneider, J., Marín-Samper, L., Arístegui, J., Renforth, P.,  
1568 Taucher, J., and Riebesell, U.: Stability of alkalinity in ocean alkalinity enhancement (OAE)  
1569 approaches - consequences for durability of CO<sub>2</sub> storage, *Biogeosciences*, 20, 781-802,  
1570 <https://doi.org/10.5194/bg-20-781-2023>, 2023.

1571 Harvey, L. D. D.: Mitigating the atmospheric CO<sub>2</sub> increase and ocean acidification by adding  
1572 limestone powder to upwelling regions, *J. Geophys. Res.*, 113, C4,  
1573 <https://doi.org/10.1029/2007JC004373>, 2008.

1574 He, J., and Tyka, M. D.: Limits and CO<sub>2</sub> equilibration of near-coast alkalinity enhancement,  
1575 *Biogeosciences*, 20, 27–43, <https://doi.org/10.5194/bg-20-27-2023>, 2023.

1576 Heuzé, C.: Antarctic Bottom Water and North Atlantic Deep Water in CMIP6 models, *Ocean*  
1577 *Sci.*, 17, 59–90, <https://doi.org/10.5194/os-17-59-2021>, 2021.

1578 Hinrichs, C., Köhler, P., Völker, C., and Hauck, J.: Alkalinity biases in CMIP6 Earth System  
1579 Models and implications for simulated CO<sub>2</sub> drawdown via artificial alkalinity enhancement,  
1580 *Biogeosci. Discuss.*, <https://doi.org/10.5194/bg-2023-26>, 2023.

1581 Ho, D. T., Bopp, L., Palter, J. B., Long, M. C., Boyd, P., Neukermans, G., and Bach, L.:  
1582 Monitoring, Reporting, and Verification for Ocean Alkalinity Enhancement, in: Guide to Best  
1583 Practices in Ocean Alkalinity Enhancement Research (OAE Guide 23), edited by: Oschlies, A.,  
1584 Stevenson, A., Bach, L., Fennel, K., Rickaby, R., Satterfield, T., Webb, R., and Gattuso, J.-P.,  
1585 Copernicus Publications, State Planet, <https://doi.org/10.-XXXXX>, 2023.

1586 Hoffman, R. N. and Atlas, R.: Future observing system simulation experiments, *B. Am.*  
1587 *Meteorol. Soc.*, 97, 1601–1616, <https://doi.org/10.1175/BAMS-D-15-00200.1>, 2016.

1588 House, K. Z., House, C. H., Schrag, D. P., and Aziz, M. J.: Electrochemical acceleration of  
1589 chemical weathering for carbon capture and sequestration, *Enrgy. Proced.*, 1, 4953-4960,  
1590 <https://doi.org/10.1016/j.egypro.2009.02.327>, 2009.

1591 Hu, J., Fennel, K., Mattern, J. P., and Wilkin, J.: Data assimilation with a local Ensemble Kalman  
1592 Filter applied to a three-dimensional biological model of the Middle Atlantic Bight,  
1593 *J. Marine Syst.*, 94, 145-156, <https://doi.org/j.jmarsys.2011.11.016>, 2012.

1594 Huettel, M., Berg, P., and Kostka, J. E.: Benthic exchange and biogeochemical cycling in  
1595 permeable sediments, *Ann. Rev. Mar. Sci.*, 6, 23–51, <https://doi.org/10.1146/annurev-marine-051413-012706>, 2014.

1597 Ilyina, T., Wolf-Gladrow, D., Munhoven, G., and Heinze, C.: Assessing the potential of calcium-  
1598 based artificial ocean alkalization to mitigate rising atmospheric CO<sub>2</sub> and ocean acidification,  
1599 *Geophys. Res. Lett.*, 40, 5909-5914, <https://doi.org/10.1002/2013GL057981>, 2013.

1600 IPCC: Climate Change 2013: The Physical Science Basis, Contribution of Working Group I to the  
1601 Fifth Assessment Report of the Intergovernmental Panel on Climate Change, edited by: Stocker,  
1602 T. F., Qin, D., Plattner, G.-K., Tignor, M., Allen, S. K., Boschung, J., Nauels, A., Xia, Y., Bex, V.,  
1603 Midgley, P. M., Cambridge University Press, 1585 pp., ISBN 978-92-9169-138-8, 2013.

1604 Jahnke, R. A.: Global synthesis, in: Carbon and nutrient fluxes in continental margins: A global  
1605 synthesis, edited by: Liu, K.-K., Atkinson, L., Quiñones, R., and Talaue-McManus, L., Springer,  
1606 Berlin, Heidelberg, Germany, 597–615, <https://doi.org/10.1007/978-3-540-92735-8>, 2010.

1607 Jirka, G. H., Doneker, R. L., and Hinton, S. W.: User’s manual for CORMIX: A hydrodynamic  
1608 mixing zone model and decision support system for pollutant discharges into surface waters, U.  
1609 S. Environmental Protection Agency, Washington, D. C., 1996.

1610 Juckes, M., Taylor, K. E., Durack, P. J., Lawrence, B., Mizielinski, M. S., Pamment, A.,  
1611 Peterschmitt, J.-Y., Rixen, M., and Sényesi, S.: The CMIP6 Data Request (DREQ, version 01.00.31),  
1612 *Geosci. Model Dev.*, 13, 201–224, <https://doi.org/10.5194/gmd-13-201-2020>, 2020.

1613 Keller, D. P., Oschlies, A., and Eby, M.: A new marine ecosystem model for the University of  
1614 Victoria Earth System Climate Model, *Geosci. Model Dev.*, 5, 1195–1220,  
1615 <https://doi.org/10.5194/gmd-5-1195-2012>, 2012.

1616 Keller, D. P., Feng, E. Y., and Oschlies, A.: Potential climate engineering effectiveness and side  
1617 effects during a high carbon dioxide-emission scenario, *Nat. Commun.*, 5, 3304,  
1618 <https://doi.org/10.1038/ncomms4304>, 2014.

1619 Keller, D. P., Lenton, A., Scott, V., Vaughan, N. E., Bauer, N., Ji, D., Jones, C. D., Kravitz, B.,  
1620 Muri, H., and Zickfeld, K.: The Carbon Dioxide Removal Model Intercomparison Project  
1621 (CDRMIP): rationale and experimental protocol for CMIP6, *Geosci. Model Dev.*, 11, 1133–1160,  
1622 <https://doi.org/10.5194/gmd-11-1133-2018>, 2018

1623 Kitagawa, G.: A self-organizing state-space model. *J. Am. Stat. Assoc.*, 93, 1203–1215,  
1624 <https://doi.org/10.2307/2669862>, 1998.

1625 Ko, Y. H., Lee, K., Eom, K. H., and Han, I.-S.: Organic alkalinity produced by phytoplankton  
1626 and its effect on the computation of ocean carbon parameters, *Limnol. Oceanogr.*, 61, 1462-1471,  
1627 <https://doi.org/10.1002/lno.10309>, 2016.

1628 Koeve, W., and Oschlies, A.: Potential impact of DOM accumulation on fCO<sub>2</sub> and carbonate ion  
1629 computations in ocean acidification experiments, *Biogeosciences*, 9, 3787-3798,  
1630 <https://doi.org/10.5194/bg-9-3787-2012>, 2012.

1631 Köhler, P., Hartmann, J., and Wolf-Gladrow, D. A.: Geoengineering potential of artificially  
1632 enhanced silicate weathering of olivine, *Proc. Natl. Acad. Sci. U. S. A.*, 107, 20228-20233,  
1633 <https://doi.org/10.1073/pnas.1000545107>, 2010.

1634 Köhler, P., Abrams, J. F., Völker, C., Hauck, J., and Wolf-Gladrow, D. A.: Geoengineering  
1635 impact of open ocean dissolution of olivine on atmospheric CO<sub>2</sub>, surface ocean pH and marine  
1636 biology, *Environ. Res. Lett.*, 8, 014009, <https://doi.org/10.1088/1748-9326/8/1/014009>, 2013.

1637 Krumhardt, K. M., Lovenduski, N. S., Iglesias-Rodriguez, M. D., and Lkeypas, J. A.:  
1638 Coccolithophore growth and calcification in a changing ocean, *Prog. Oceanogr.*, 159, 276-295,  
1639 <https://doi.org/10.1016/j.pocean.2017.10.007>, 2017.

1640 Laurent, A., Fennel, K., Wilson, R., Lehrter, J., and Devereux, R.: Parameterization of  
1641 biogeochemical sediment–water fluxes using in situ measurements and a diagenetic model,  
1642 *Biogeosciences*, 13, 77-94, <https://doi.org/10.5194/bg-13-77-2016>, 2016.

1643 Laurent, A., Fennel, K., and Kuhn, A.: An observation-based evaluation and ranking of  
1644 historical Earth system model simulations in the northwest North Atlantic Ocean,  
1645 *Biogeosciences*, 18, 1803–1822, <https://doi.org/10.5194/bg-18-1803-2021>, 2021.

1646 Laurent, A., Wang, B., Pei, A., Ohashi, K., Sheng, J., Garcia Larez, E., Fradette, C., Rakshit, S.,  
1647 Atamanchuk, D., Azetsu-Scott, K., Algar, C., Wallace, D., Burt, W., and K. Fennel: A high-  
1648 resolution nested model to study the effects of alkalinity additions in a mid-latitude coastal  
1649 fjord, Abstract number: 1486172, presented at the Ocean Sciences Meeting 2024, 18-23 February  
1650 2024.

1651 Lellouche, J.-M., Greiner, E., Bourdallé-Badie, R., Garric, G., Melet, A., Dréville, M., Bricaud,  
1652 C., Hamon, M., Le Galloudec, O., Regnier, C., Candela, T., Testut, C.-E., Gasparin, F., Ruggiero,  
1653 G., Benkiran, M., Drillet, Y., and Le Traon, P.-Y.: The Copernicus Global 1/12° Oceanic and Sea  
1654 Ice GLORYS12 Reanalysis, *Front. Earth Sci.*, 9, 698876, <https://doi.org/10.3389/feart.2021.698876>,  
1655 2021.

1656 Lewis, E. R., and Wallace, D. W. R.: Program developed for CO2 system calculations,  
1657 Environmental System Science Data Infrastructure for a Virtual Ecosystem (ESS-DIVE), United  
1658 States, <https://doi.org/10.15485/1464255>, 1998.

1659 Li, G., Iskandarani, M., Le Hénaff, M., Winokur, J., Le Maître, O. P., and Knio, O. M.:  
1660 Quantifying initial and wind forcing uncertainties in the Gulf of Mexico, *Computat. Geosci.*, 20,  
1661 1133-1153, <https://doi.org/10.1007/s10596-016-9581-4>, 2016.

1662 Liang, J.-H., McWilliams, J. C., Sullivan, P. P., and Baschek, B.: Modeling bubbles and dissolved  
1663 gases in the ocean, *J. Geophys. Res.-Oceans*, 116, C3, <https://doi.org/10.1029/2010JC006579>, 2011.

1664 Liang, J.-H., Deutsch, C., McWilliams, J. C., Baschek, B., Sullivan, P. P., and Chiba, D.:  
1665 Parameterizing bubble-mediated air-sea gas exchange and its effect on ocean ventilation, *Global  
1666 Biogeochem. Cy.*, 27, 894-905, <https://doi.org/10.1002/gbc.20080>, 2013.

1667 Lohrenz, S. E., Cai, W.-J., Chakraborty, S., Huang, W.-J., Guo, X., He, R., Xue, Z., Fennel, K.,  
1668 Howden, S., and Tian, H.: Satellite estimation of coastal pCO<sub>2</sub> and air-sea flux of carbon dioxide  
1669 in the northern Gulf of Mexico, *Remote Sens. Environ.*, 207, 71-83,  
1670 <https://doi.org/10.1016/j.rse.2017.12.039>, 2018.

1671 Long, J. S., Hu, C., Robbins, L. L., Byrne, R. H., Paul, J. H., and Wolny, J. L.: Optical and  
1672 biochemical properties of a southwest Florida whiting event, *Estuar. Coast. Shelf S.*, 196, 258-  
1673 268, <https://doi.org/10.1016/j.ecss.2017.07.017>, 2017.

1674 Long, M. C., Moore, J. K., Lindsay, K., Levy, M., Doney, S. C., Luo, J. Y., Krumhardt, K. M.,  
1675 Letscher, R. T., Grover, M., and Sylvester, Z. T.: Simulations with the marine biogeochemistry  
1676 library (MARBL), *J. Adv. Model. Earth Syst.*, <https://doi.org/10.1029/2021ms002647>, 2021.

1677 Mattern, J.P., Fennel, K., and Dowd, M.: Estimating time-dependent parameters for a biological  
1678 ocean model using an emulator approach, *J. Mar. Syst.*, 96–97, 32-47,  
1679 <https://doi.org/10.1016/j.jmarsys.2012.01.015>, 2012.

1680 Mattern, J. P., Fennel, K., and Dowd, M.: Periodic time-dependent parameters improving  
1681 forecasting abilities of biological ocean models, *Geophys. Res. Lett.*, 41, 6848-6854,  
1682 <https://doi.org/10.1002/2014GL061178>, 2014.

1683 Mattern, J. P., Song, H., Edwards, C. A., Moore, A. M., and Fiechter, J.: Data assimilation of  
1684 physical and chlorophyll observations in the California Current System using two  
1685 biogeochemical models, *Ocean Model.*, 109, 55–71, <https://doi.org/10.1016/j.ocemod.2016.12.002>,  
1686 2017.

1687 Maurer, T. L., Plant, J. N., and Johnson, K. S.: Delayed-Mode Quality Control of Oxygen,  
1688 Nitrate, and pH Data on SOCCOM Biogeochemical Profiling Floats, *Front. Mar. Sci.*, 8,  
1689 <https://doi.org/10.3389/fmars.2021.683207>, 2021.

1690 McLaughlin, K., Weisberg, S. B., Dickson, A. G., Hofmann, G., Newton, J. A., Aseltine-Neilson,  
1691 D., Barton, A., Cudd, S., Feely, R. A., Jefferds, I. W., Jewett, E. B., King, T., Langdon, C. J.,  
1692 McAfee, S., Pleschner-Steele, D., and Steele, B.: Core principles of the California current  
1693 acidification network: Linking chemistry, physics, and ecological effects, *Oceanography*, 28,  
1694 160-169, <http://www.jstor.org/stable/24861878>, 2015.

1695 Mengis, N., Keller, D. P., MacDougall, A. H., Eby, M., Wright, N., Meissner, K. J., Oschlies, A.,  
1696 Schmittner, A., MacIsaac, A. J., Matthews, H. D., and Zickfeld, K.: Evaluation of the University  
1697 of Victoria Earth System Climate Model version 2.10 (UVic ESCM 2.10), *Geosci. Model Dev.*, 13,  
1698 4183–4204, <https://doi.org/10.5194/gmd-13-4183-2020>, 2020.

1699 Mensa, J. A., Özgökmen, T. M., Poje, A. C., and Imberger, J.: Material transport in a convective  
1700 surface mixed layer under weak wind forcing, *Ocean Model.*, 96, 226-242,  
1701 <https://doi.org/10.1016/j.ocemod.2015.10.006>, 2015.

1702 Meysman, F. J. R., Middelburg, J. J., and Heip, C. H. R.: Bioturbation: a fresh look at Darwin's  
1703 last idea, *Trends Ecol. Evol.*, 21, 688-695, <https://doi.org/10.1016/j.tree.2006.08.002>, 2006.

1704 Meysman, F. J. R., and Montserrat, F.: Negative CO<sub>2</sub> emissions via enhanced silicate weathering  
1705 in coastal environments, *Biol. Lett.*, 13, 20160905, <http://doi.org/10.1098/rsbl.2016.0905>, 2017.

1706 Middelburg, J. J., Soetaert, K., and Hagens, M.: Ocean Alkalinity, Buffering and Biogeochemical  
1707 Processes, *Rev. Geophys.*, 58, e2019RG000681, <https://doi.org/10.1029/2019RG000681>, 2020.

1708 Millero, F. J.: The Marine Inorganic Carbon Cycle, *Chem. Rev.*, 107, 308-341,  
1709 <https://doi.org/10.1021/cr0503557>, 2007.

1710 Mongin, M., Baird, M. E., Tilbrook, B., Matear, R. J., Lenton, A., Herzfeld, M., Wild-Allen, K.,  
1711 Skerratt, J., Margvelashvili, N., Robson, B. J., Duarte, C. M., Gustafsson, M. S. M., Ralph, P. J.,  
1712 and Steven, A. D. L.: The exposure of the Great Barrier Reef to ocean acidification, *Nat.*  
1713 *Commun.*, 7, 10732, <https://doi.org/10.1038/ncomms10732>, 2016.

1714 Mongin, M., Baird, M. E., Lenton, A., Neill, C., and Akl, J.: Reversing ocean acidification along  
1715 the Great Barrier Reef using alkalinity injection, *Environ. Res. Lett.*, 16, 064068,  
1716 <https://doi.org/10.1088/1748-9326/ac002d>, 2021.

1717 Montserrat, F., Renforth, P., Hartmann, J., Leermakers, M., Knops, P., and Meysman, F. J. R.:  
1718 Olivine dissolution in seawater: Implications for CO<sub>2</sub> sequestration through enhanced  
1719 weathering in coastal environments, *Environ. Sci. Technol.*, 51, 3960-3972,  
1720 <https://doi.org/10.1021/acs.est.6b05942>, 2017.

- 1721 Moras, C. A., Bach, L. T., Cyronak, T., Joannes-Boyau, R., and Schulz, K. G.: Ocean alkalinity  
1722 enhancement – avoiding runaway CaCO<sub>3</sub> precipitation during quick and hydrated lime  
1723 dissolution, *Biogeosciences*, 19, 3537–3557, <https://doi.org/10.5194/bg-19-3537-2022>, 2022.
- 1724 Moriarty, J. M., Harris, C. K., Fennel, K., Friedrichs, M. A. M., Xu, K., and Rabouille, C.: The  
1725 roles of resuspension, diffusion and biogeochemical processes on oxygen dynamics offshore of  
1726 the Rhône River, France: a numerical modeling study, *Biogeosciences*, 14, 1919-1946,  
1727 <https://doi.org/10.5194/bg-14-1919-2017>, 2017.
- 1728 Moriarty, J.M., Harris, C. K., Friedrichs, M. A. M., Fennel, K., and Xu, K.: Impact of seabed  
1729 resuspension on oxygen and nitrogen dynamics in the northern Gulf of Mexico: A numerical  
1730 modeling study, *J. Geophys. Res-Oceans*, 123, 7237-7263, <https://doi.org/10.1029/2018JC013950>,  
1731 2018.
- 1732 Morse, J. W., Mucci, A., and Millero, F. J.: The solubility of calcite and aragonite in seawater of  
1733 35‰ salinity at 25°C and atmospheric pressure, *Geochim. Cosmochim. Ac.*, 44, 85-94,  
1734 [https://doi.org/10.1016/0016-7037\(80\)90178-7](https://doi.org/10.1016/0016-7037(80)90178-7), 1980.
- 1735 Mu, L., Palter, J. B., and Wang, H.: Considerations for hypothetical carbon dioxide removal via  
1736 alkalinity addition in the Amazon River watershed, *EGUsphere* [preprint],  
1737 <https://doi.org/10.5194/egusphere-2022-1505>, 2023.
- 1738 Naveira Garabato, A. C., MacGilchrist, G. A., Brown, P. J., Evans, D. G., Meijers, A. J. S., and  
1739 Zika, J. D.: High-latitude ocean ventilation and its role in Earth’s climate transitions, *Philos.*  
1740 *Trans. A Math. Phys. Eng. Sci.*, 375, <https://doi.org/10.1098/rsta.2016.0324>, 2017.
- 1741 Negrete-García, G., Luo, J. Y., Long, M. C., Lindsay, K., Levy, M., and Barton, A. D.: Plankton  
1742 energy flows using a global size-structured and trait-based model, *Prog. Oceanogr.*, 209, 102898,  
1743 <https://doi.org/10.1016/j.pocan.2022.102898>, 2022.
- 1744 Oschlies, A.: Impact of atmospheric and terrestrial CO<sub>2</sub> feedbacks on fertilization-induced  
1745 marine carbon uptake, *Biogeosciences*, 6, 1603–1613, <https://doi.org/10.5194/bg-6-1603-2009>,  
1746 2009.
- 1747 Paquay, F. S., and Zeebe, R. E.: Assessing possible consequences of ocean liming on ocean pH,  
1748 atmospheric CO<sub>2</sub> concentration and associated costs, *Int. J. Green. Gas Con.*, 17, 183-188,  
1749 <https://doi.org/10.1016/j.ijggc.2013.05.005>, 2013.
- 1750 Pascoe, C., Lawrence, B. N., Guilyardi, E., Juckes, M., and Taylor, K. E.: Documenting numerical  
1751 experiments in support of the Coupled Model Intercomparison Project Phase 6 (CMIP6), *Geosci.*  
1752 *Model Dev.*, 13, 2149–2167, <https://doi.org/10.5194/gmd-13-2149-2020>, 2020.
- 1753 Paul, A. J., and Bach, L. T.: Universal response pattern of phytoplankton growth rates to  
1754 increase CO<sub>2</sub>, *New Phytol.*, 228, 1710-1716, <https://doi.org/10.1111/nph.16806>, 2020.

- 1755 Paulmier, A., Kriest, I., and Oschlies, A.: Stoichiometries of remineralisation and denitrification  
1756 in global biogeochemical ocean models, *Biogeosciences*, 6, 923–935, [https://doi.org/10.5194/bg-6-](https://doi.org/10.5194/bg-6-923-2009)  
1757 923-2009, 2009.
- 1758 Petrie, R., Denvil, S., Ames, S., Levavasseur, G., Fiore, S., Allen, C., Antonio, F., Berger, K.,  
1759 Bretonnière, P.-A., Cinquini, L., Dart, E., Dwarakanath, P., Druken, K., Evans, B., Franchistéguy,  
1760 L., Gardoll, S., Gerbier, E., Greenslade, M., Hassell, D., Iwi, A., Juckes, M., Kindermann, S.,  
1761 Lacinski, L., Mirto, M., Nasser, A. B., Nassisi, P., Nienhouse, E., Nikonov, S., Nuzzo, A.,  
1762 Richards, C., Ridzwan, S., Rixen, M., Serradell, K., Snow, K., Stephens, A., Stockhause, M.,  
1763 Vahlenkamp, H., and Wagner, R.: Coordinating an operational data distribution network for  
1764 CMIP6 data, *Geosci. Model Dev.*, 14, 629–644, <https://doi.org/10.5194/gmd-14-629-2021>, 2021.
- 1765 Raimondi, L., Matthews, J. B. R., Atamanchuk, D., Azetsu-Scott, K., and Wallace, D. W. R.: The  
1766 internal consistency of the marine carbon dioxide system for high latitude shipboard and *in situ*  
1767 monitoring, *Mar. Chem.*, 213, 49-70, <https://doi.org/10.1016/j.marchem.2019.03.001>, 2019.
- 1768 Ramadhan, A., Wagner, G., Hill, C., Campin, J.-M., Churavy, V., Besard, T., Souza, A., Edelman,  
1769 A., Ferrari, R., and Marshall, J.: Oceananigans.jl: Fast and friendly geophysical fluid dynamics in  
1770 GPUs, *J. Open Source Softw.*, 5, <https://doi.org/10.21105/joss.02018>, 2020.
- 1771 Rau, G. H., McLeod, E. L., and Hoegh-Guldberg, O.: The need for new ocean conservation  
1772 strategies in a high-carbon dioxide world, *Nat. Clim. Change*, 2, 720-724,  
1773 <https://doi.org/10.1038/nclimate1555>, 2012.
- 1774 Renforth, P., and Henderson, G.: Assessing ocean alkalinity for carbon sequestration, *Rev.*  
1775 *Geophys.*, 55, 636–674, <https://doi.org/10.1002/2016RG000533>, 2017.
- 1776 Riebesell, U., Wold-Gladrow, D. A., and Smetacek, V.: Carbon dioxide limitation of marine  
1777 phytoplankton growth rates, *Nature*, 361, 249-251, <https://doi.org/10.1038/361249a0>, 1993.
- 1778 Ringham, M.: High resolution, in-situ studies of seawater carbonate chemistry and carbon  
1779 cycling in costal systems using CHANnelized Opticals System II, Ph. D. thesis, Massachusetts  
1780 Institute of Technology, 127 pp., <https://hdl.handle.net/1721.1/144860>, 2022.
- 1781 Rothstein, L. M., Cullen, J. J., Abbott, M., Chassignet, E. P., Denman, K., Doney, S. C., Ducklow,  
1782 H., Fennel, K., Follows, M., Haidvogel, D., Hofmann, E., Karl, D. M., Kindle, J., Lima, I.,  
1783 Maltrud, M., McClain, C., McGillicuddy, D., Olascoaga, M. J., Spitz, Y., Wiggert, J., and Woder,  
1784 J.: Modeling Ocean Ecosystems: The PARADIGM Program, *Oceanography*, 19, 22-51,  
1785 <https://doi.org/10.5670/oceanog.2006.89>, 2015.
- 1786 Rutherford, K., Fennel, K., Atamanchuk, D., Wallace, D., and Thomas, H.: A modelling study of  
1787 temporal and spatial pCO<sub>2</sub> variability on the biologically active and temperature-dominated  
1788 Scotian Shelf, *Biogeosciences*, 18, 6271-6286, <https://doi.org/10.5194/bg-18-6271-2021>, 2021.
- 1789 Sarmiento, J. L., and Gruber, N.: *Ocean Biogeochemical Dynamics*, Princeton University Press,  
1790 <https://doi.org/10.2307/j.ctt3fgxqx>, 2006.



1791 Sauerland, V., Kriest, I., Oschlies, A., and Srivastav, A.: Multiobjective calibration of a global  
1792 biogeochemical ocean model against nutrients, oxygen, and oxygen minimum zones, *J. Adv.*  
1793 *Model. Earth Sy.*, 11, 1285–1308, <https://doi.org/10.1029/2018MS001510>, 2019.

1794 Schartau, M., Wallhead, P., Hemmings, J., Löptien, U., Kriest, I., Krishna, S., Ward, B. A.,  
1795 Slawig, T., and Oschlies, A.: Reviews and syntheses: parameter identification in marine  
1796 planktonic ecosystem modelling, *Biogeosciences*, 14, 1647–1701, [https://doi.org/10.5194/bg-14-](https://doi.org/10.5194/bg-14-1647-2017)  
1797 1647-2017, 2017.

1798 Schmittner, A., Oschlies, A., Matthews, H. D., and Galbraith, E. D.: Future changes in climate,  
1799 ocean circulation, ecosystems, and biogeochemical cycling simulated for a business-as-usual  
1800 CO<sub>2</sub> emission scenario until 4000 AD, *Global Biogeochem. Cy.*, 22,  
1801 <https://doi.org/10.1029/2007GB002953>, 2008.

1802 Schulz, K. G., Bach, L. T., and Dickson, A. G.: Seawater carbonate system considerations for  
1803 ocean alkalinity enhancement research, in: *Guide to Best Practices in Ocean Alkalinity*  
1804 *Enhancement Research (OAE Guide 23)*, edited by: Oschlies, A., Stevenson, A., Bach, L., Fennel,  
1805 K., Rickaby, R., Satterfield, T., Webb, R., and Gattuso, J.-P., Copernicus Publications, State  
1806 Planet, <https://doi.org/10.-XXXXX>, 2023.

1807 Seitzinger, S. P., Harrison, J. A., Böhlke, J. K., Bouwman, A. F., Lowrance, R., Tobias, C., and  
1808 Van Drecht, G.: Denitrification across landscapes and waterscapes: A synthesis, *Ecol. Appl.*, 16,  
1809 2064–2090, [https://doi.org/10.1890/1051-0761\(2006\)016\[2064:DALAWA\]2.0.CO;2](https://doi.org/10.1890/1051-0761(2006)016[2064:DALAWA]2.0.CO;2), 2006.

1810 Seitzinger, S. P., Mayorga, E., Bouwman, A. F., Kroeze, C., Beusen, H. W., Billen, G., Van Dracht,  
1811 G., Dumont, E., Fekete, B. M., Garnier, J., and Harrison, J. A.: Global river nutrient export: A  
1812 scenario analysis of past and future trends, *Global Biogeochem. Cycles*, 24, GB0A08,  
1813 <https://doi.org/10.1029/2009GB003587>, 2010.

1814 Shangquan, Q., Prody, A., Wirth, T. S., Briggs, E. M., Martz, T. R., and DeGrandpre, M. D.: An  
1815 inter-comparison of autonomous *in situ* instruments for ocean CO<sub>2</sub> measurements under  
1816 laboratory-controlled conditions, *Mar. Chem.*, 240, 104085,  
1817 <https://doi.org/10.1016/j.marchem.2022.104085>, 2022.

1818 Shchepetkin, A. F., and McWilliams, J. C.: The regional oceanic modeling system (ROMS): a  
1819 split-explicit, free-surface, topography-following-coordinate oceanic model, *Ocean Model.*, 9,  
1820 347-404, <https://doi.org/10.1016/j.ocemod.2004.08.002>, 2005.

1821 Smagorinsky, J.: General circulation experiments with the primitive equations, *Mon. Weather*  
1822 *Rev.*, 91, 99-164, [https://doi.org/10.1175/1520-0493\(1963\)091<0099:GCEWTP>2.3.CO;2](https://doi.org/10.1175/1520-0493(1963)091<0099:GCEWTP>2.3.CO;2), 1963.

1823 Smith, K. M., Hamlington, P. E., Niemeyer, K. E., Fox-Kemper, B., and Lovenduski, N. S.: Effects  
1824 of Langmuir turbulence on upper ocean carbonate chemistry, *J. Adv. Model. Earth Sy.*, 10, 3030-  
1825 3048, <https://doi.org/10.1029/2018MS001486>, 2018.

1826 Soetaert, K., Hofmann, A. F., Middelburg, J. J., Meysman, F. J. R., and Greenwood, J.: The effect  
1827 of biogeochemical processes on pH, *Mar. Chem.*, 105, 30-51,  
1828 <https://doi.org/10.1016/j.marchem.2006.12.012>, 2007.

1829 Sonnichsen, C., Atamanchuk, D., Hendricks, A., Morgan, S., Smith, J., Grundke, I., Luy, E., and  
1830 Sieben, V. J.: An Automated Microfluidic Analyzer for in-situ Monitoring of Total Alkalinity,  
1831 *ACS Sens.*, 8, 344-352, <https://doi.org/10.1021/acssensors.2c02343>, 2023.

1832 Stammer, D.: Global Characteristics of Ocean Variability Estimated from Regional  
1833 TOPEX/POSEIDON Altimeter Measurements, *J. Phys. Oceanogr.*, 27, 1743–1769,  
1834 [https://doi.org/10.1175/1520-0485\(1997\)027<1743:GCOOVE>2.0.CO;2](https://doi.org/10.1175/1520-0485(1997)027<1743:GCOOVE>2.0.CO;2), 1997.

1835 Stow, C. A., Jolliff, J., McGillicuddy Jr., D. J., Doney, S. C., Allen, J. I., Friedrichs, M. A. M., Rose,  
1836 K. A., and Wallhead, P.: Skill assessment for coupled biological/physical models of marine  
1837 systems, *J. Mar. Syst.*, 76, 4-15, <https://doi.org/10.1016/j.jmarsys.2008.03.011>, 2009.

1838 Subhas, A. V., Lehmann, N., and Rickaby, R.: Natural Analogs to Ocean Alkalinity  
1839 Enhancement, in: *Guide to Best Practices in Ocean Alkalinity Enhancement Research (OAE*  
1840 *Guide 23)*, edited by: Oschlies, A., Stevenson, A., Bach, L., Fennel, K., Rickaby, R., Satterfield, T.,  
1841 Webb, R., and Gattuso, J.-P., Copernicus Publications, State Planet, <https://doi.org/10.-XXXXX>,  
1842 2023.

1843 Subhas, A. V., Dong, S., Naviaux, J. D., Rollins, N. E., Ziveri, P., Gray, W., Rae, J. W. B., Liu, X.,  
1844 Bryne, R. H., Chen, S., Moore, C., Martell-Bonnet, L., Steiner, Z., Antler, G., Hu, H., Lunstrum,  
1845 A., Hou, Y., Kemnits, N., Stutsman, J., Pallacks, S., Dugenne, M., Quay, P. D., Berelson, W. M.,  
1846 and Adkins, J. F.: Shallow calcium carbonate cycling in the North Pacific Ocean, *Global*  
1847 *Biogeochem. Cy.*, 36, e2022GB007388, <https://doi.org/10.1029/2022GB007388>, 2022.

1848 Sulpis, O., Jeansseon, E., Dinauer, A., Lauvset, S. K., and Middelburg, J. J.: Calcium carbonate  
1849 dissolution patterns in the ocean, *Nat. Geosci.*, 14, 423-428, [https://doi.org/10.1038/s41561-021-](https://doi.org/10.1038/s41561-021-00743-y)  
1850 [00743-y](https://doi.org/10.1038/s41561-021-00743-y), 2021.

1851 Takeshita, Y., Jones, B. D., Johnson, K. S., Chavez, F. P., Rudnick, D. L., Blum, M., Conner, K.,  
1852 Jensen, S., Long, J. S., Maughan, T., Mertz, K. L., Sherman, J. T., and Warren, J. K.: Accurate pH  
1853 and O<sub>2</sub> Measurements from Spray Underwater Gliders, *J. Atmos. Oceanic Technol.*, 38, 181–195,  
1854 <https://doi.org/10.1175/JTECH-D-20-0095.1>, 2021.

1855 Taylor, L. L., Quirk, J., Thorley, R. M. S., Kharecha, P. A., Hansen, J., Ridgwell, A., Lomas, M. R.,  
1856 Banwart, S. A., and Beerling, D. J.: Enhanced weathering strategies for stabilizing climate and  
1857 averting ocean acidification, *Nat. Clim. Change*, 6, 402-406,  
1858 <https://doi.org/10.1038/nclimate2882>, 2016.

1859 Taylor, J. R., Smith, K. M., and Vreugdenhil, C. A.: The influence of submesoscales and vertical  
1860 mixing on the export of sinking tracers in Large-Eddy Simulations, *J. Phys. Oceanogr.*, 50, 1319-  
1861 1339, <https://doi.org/10.1175/JPO-D-19-0267.1>, 2020.

- 1862 Teruzzi, A., Bolzon, G., Salon, S., Lazzari, P., Solidoro, C., and Cossarini, G.: Assimilation of  
1863 coastal and open sea biogeochemical data to improve phytoplankton simulation in the  
1864 Mediterranean Sea, *Ocean Modell*, 132, 46–60, <https://doi.org/10.1016/j.ocemod.2018.09.007>,  
1865 2018.
- 1866 Thacker, W. C.: The role of the Hessian matrix in fitting models to measurements, *J. Geophys.*  
1867 *Res.-Oceans*, 95, 6177-6196, <https://doi.org/10.1029/JC094iC05p06177>, 1989.
- 1868 Thacker, W. C., Srinivasan, A., Iskandarani, M., Knio, O. M., and Le Hénaff, M.: Propagating  
1869 boundary uncertainties using polynomial expansions, *Ocean Model.*, 43-44, 52-63,  
1870 <https://doi.org/10.1016/j.ocemod.2011.11.011>, 2012.
- 1871 Turner, K. E., Smith, D. M., Katavouta, A., and Williams, R. G.: Reconstructing ocean carbon  
1872 storage with CMIP6 Earth system models and synthetic Argo observations, *Biogeosciences*, 20,  
1873 1671-1690, <https://doi.org/10.5194/bg-20-1671-2023>, 2023.
- 1874 Verdy, A., and Mazloff, M. R.: A data assimilating model for estimating Southern Ocean  
1875 biogeochemistry, *J. Geophys. Res.*, 122, 6968–6988, <https://doi.org/10.1002/2016JC012650>, 2017.
- 1876 Waliser, D., Gleckler, P. J., Ferraro, R., Taylor, K. E., Ames, S., Biard, J., Bosilovich, M. G.,  
1877 Brown, O., Chepfer, H., Cinquini, L., Durack, P. J., Eyring, V., Mathieu, P.-P., Lee, T., Pinnock,  
1878 S., Potter, G. L., Rixen, M., Saunders, R., Schulz, J., Thépaut, J.-N., and Tuma, M.: Observations  
1879 for Model Intercomparison Project (Obs4MIPs): status for CMIP6, *Geosci. Model Dev.*, 13, 2945–  
1880 2958, <https://doi.org/10.5194/gmd-13-2945-2020>, 2020.
- 1881 Wang, B., Fennel, K., Yu, L., and Gordon, C.: Assessing the value of biogeochemical Argo  
1882 profiles versus ocean color observations for biogeochemical model optimization in the Gulf of  
1883 Mexico, *Biogeosciences*, 17, 4059–4074, <https://doi.org/10.5194/bg-17-4059-2020>, 2020.
- 1884 Wang, B., Laurent, A., and K. Fennel: Numerical dye tracer experiments in Bedford Basin in  
1885 support of Ocean Alkalinity Enhancement research, Abstract number: 1479880, presented at the  
1886 Ocean Sciences Meeting 2024, 18-23 February 2024.
- 1887 Wang, H., Pilcher, D. J., Kearney, K. A., Cross, J. N., Shugart, O. M., Eisaman, M. D., and Carter,  
1888 B. R.: Simulated impact of ocean alkalinity enhancement on atmospheric CO<sub>2</sub> removal in the  
1889 Bering Sea, *Earths Future*, 11, <https://doi.org/10.1029/2022ef002816>, 2023.
- 1890 Wang, Z. A., Sonnichsen, F. N., Bradley, A. M., Hoering, K. A., Lanagan, T. M., Chu, S. N.,  
1891 Hammar, T. R., and Camilli, R.: In situ sensor technology for simultaneous spectrophotometric  
1892 measurements of seawater total dissolved inorganic carbon and pH, *Environ. Sci. Technol.*, 49,  
1893 4441-4449, <https://doi.org/10.1021/es504893n>, 2015.
- 1894 Wanninkhof, R.: Relationship between wind speed and gas exchange over the ocean, *J.*  
1895 *Geophys. Res.-Oceans*, 97, C5, <https://doi.org/10.1029/92JC00188>, 1992.
- 1896 Wanninkhof, R.: Relationship between wind speed and gas exchange over the ocean revisited,  
1897 *Limnol. Oceanogr. - Meth.*, 12, 351-362, <https://doi.org/10.4319/lom.2014.12.351>, 2014.

- 1898 Whitt, D. B., Lévy, M., and Taylor, J. R.: Submesoscales enhance storm-driven vertical mixing of  
1899 nutrients: insights from a biogeochemical large eddy simulation, *J. Geophys. Res.-Oceans*, 124,  
1900 8140-8165, <https://doi.org/10.1029/2019JC015370>, 2019.
- 1901 Wilcox, L. J., Allen, R. J., Samset, B. H., Bollasina, M. A., Griffiths, P. T., Keeble, J. M., Lund, M.  
1902 T., Makkonen, R., Merikanto, J., O'Donnell, D., Paynter, D. J., Persad, G. G., Rumbold, S. T.,  
1903 Takemura, T., Tsigaridis, K., Undorf, S., and Westervelt, D. M.: The Regional Aerosol Model  
1904 Intercomparison Project (RAMIP), *Geosci. Model Dev. Discuss.* [preprint],  
1905 <https://doi.org/10.5194/gmd-2022-249>, in review, 2022.
- 1906 Wolf-Gladrow, D. A., Zeebe, R. E., Klaas, C., Körtzinger, A., and Dickson, A. G.: Total alkalinity:  
1907 The explicit conservative expression and its application to biogeochemical processes, *Mar.*  
1908 *Chem.*, 106, 287-300, <https://doi.org/10.1016/j.marchem.2007.01.006>, 2007.
- 1909 Yu, L., Fennel, K., Bertino, L., Gharamti, M. E., and Thompson, K. R.: Insights on multivariate  
1910 updates of physical and biogeochemical ocean variables using an Ensemble Kalman Filter and  
1911 an idealized model of upwelling, *Ocean Model.*, 126, 13–28,  
1912 <https://doi.org/10.1016/j.ocemod.2018.04.005>, 2018.
- 1913 Zeebe, R. E., and Wolf-Gladrow, D. A.: *CO<sub>2</sub> in seawater: equilibrium, kinetics, isotopes*, Gulf  
1914 Professional Publishing, 346 pp., ISBN 9780444509468, 2001.  
1915